IMAGE: A MAP OF THE STARS OF THE ORION CONSTELLATION

Print ISSN: 2631-8490 Online ISSN: 2631-8504

JournalPreview

London Journal of Research in Science: Natural and Formal
Volume 22 | Issue 6 | Compilation 1.0

London Journals Press

Journal Content
In this Issue

London Journals Press

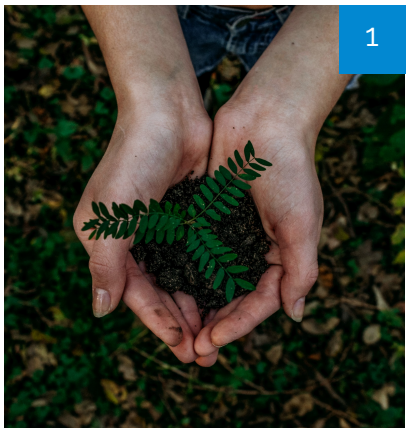

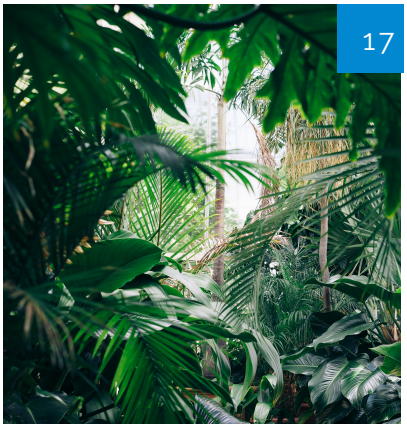

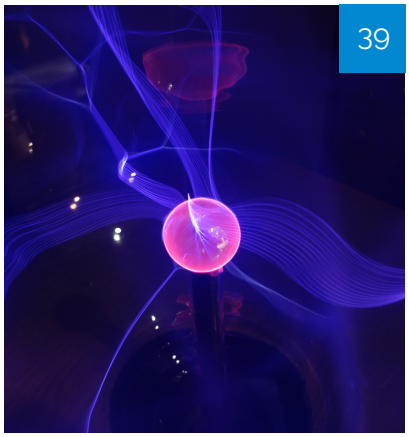

An Insulating Surface Polymeric Layer during Quenching Makes Environment Green, Increases Strength of Materials, and Decreases their Cost

Nikolai I. Kobasko

ABSTRACT

In the paper an overview on elimination of any film boiling process during quenching in Poly (Alkilene) Glycol (PAG) solutions is widely discussed. Such elimination is possible due to formation an insulating polymeric layer on the surface of quenched steel parts which decreases initial heat flux density below its critical value. An insulating polymeric layer accelerates cooling process making it uniform and very stable. In such condition, physics and mathematical interpretation of quenching technologies is reliable and creates a basis for automation and software design. The main attention in the paper is paid to mechanism of polymeric layer formation to accelerate hardening of optimal hardenability steel. All of this creates high surface compression residual stresses, makes material ductile and super strengthened, decreases steel alloying and makes possible to switch from oils and melted alkalis to low concentration of water PAG solutions. Along with quenching optimal hardenability steel, it is shown that low and high temperature mechanical treatment combined with PAG solutions as a quenchant makes environment green.

Keywords: insulating layer, film boiling elimination, accelerated cooling, strength increase, environment.

Classification: DDC Code: 620.112 LCC Code: TA407.4

Language: English

London Journals Press

LJP Copyright ID: 925691
Print ISSN: 2631-8490
Online ISSN: 2631-8504

London Journal of Research in Science: Natural and Formal

Volume 22 | Issue 6 | Compilation 1.0

An Insulating Surface Polymeric Layer during Quenching Makes Environment Green, Increases Strength of Materials, and Decreases their Cost

Nikolai I. Kobasko

ABSTRACT

In the paper an overview on elimination of any film boiling process during quenching in Poly(Alkilene) Glycol (PAG) solutions is widely discussed. Such elimination is possible due to formation an insulating polymeric layer on the surface of quenched steel parts which decreases initial heat flux density below its critical value. An insulating polymeric layer accelerates cooling process making it uniform and very stable. In such condition, physics and mathematical interpretation of quenching technologies is reliable and creates a basis for automation and software design. The main attention in the paper is paid to mechanism of polymeric layer formation to accelerate hardening of optimal hardenability steel. All of this creates high surface compression residual stresses, makes material ductile and super strengthened, decreases steel alloying and makes possible to switch from oils and melted alkalis to low concentration of water PAG solutions. Along with quenching optimal hardenability steel, it is shown that low and high temperature mechanical treatment combined with PAG solutions as a quenchant makes environment green.

Keywords: insulating layer, film boiling elimination, accelerated cooling, strength increase, environment.

Author: Intensive Technologies Ltd. Kyiv. Ukraine.

I. INTRODUCTION

As known, all machine components including cars, trucks and other small and heavy machines are heated to high temperatures and quenched in oils or water polymer solutions to provide appropriate their strength and increase service life of designed machines. In average machine components are heated to 800°C – 900°C and cooled in oils or cold-water solutions at 20°C - 30°C. The problems which arise during quenching are quench cracks, distortion, unsmooth hardness, environment pollution and so on. To prevent quench crack formation and decrease distortion, engineers in heat treating industry use slow cooling in warm and hot oils. However, slow cooling requires more alloy elements in steel to provide hardness at the core of steel parts according to required specification. The main rule in heat treating industry is hardening alloy steel in oil while plain carbon steel can be hardened in water, except high carbon steels used for special tools and dies. So, heat treating industry relates to environment pollution. During producing alloy elements from minerals needed for steel alloying additional pollution takes place. To solve this problem, in last decades intensive quenching was used [1]. It is shown that intensive quenching decreases alloying, increases service life of quenched steel parts, due to high surface compressive residual stresses super strengthening effect, reduces pollution and increases productivity [2]. However, intensive quenching productions lines are still expensive since they require powerful motors with propellers and

London Journal of Research in Science: Natural and Formal

pumps to provide sever agitation of quenchants [1]. In this paper an alternative way of performing accelerated quenching process in liquid media is discussed. Due to forming an insulating layer on the surface of hardened steel, any film boiling is eliminated that accelerates cooling process. Thus, for performing accelerated quenching in water and water solutions, several requirements should be strongly fulfilled.

- Any film boiling process during quenching in liquid medium should be absent.
- Moderate agitation of liquid should be used during quenching to provide developed transient nucleate boiling process.
- Developed transient nucleate boiling process should drop surface temperature to boiling point of a liquid within 1 – 2 seconds.

The first requirement is fulfilled if initial heat flux density during quenching is below the first critical value q_{cr1}. When initial heat flux density prevails critical value, developed film boiling takes place. When initial heat flux density q_{in} is equal to the first critical value, local film boiling process could take place that causes big distortion [3, 4]. The last is the most undesirable since local film boiling results not only in big distortion but in non-uniform hardness and crack formation.

The second requirement, moderate agitation, can be effectively fulfilled using hydrodynamic emitters that destroy film boiling via resonance effect [5].

The third requirement is fulfilled if water solutions are used to maximize critical heat flux densities [3].

Based on Provided short discussion, an accelerated and uniform cooling is designed using inverse solubility polymers [6].

II. ELIMINATION FILM BOILING BY CREATING SURFACE INSULATING LAYER

2.1 Experimental Methodology

The method for determination cooling characteristics of aqueous polymer quenchants was proposed by ASTM Standard D 6482 – 06 [7]. This test method covers the equipment and the procedure for evaluation of quenching characteristics of a quenching fluid by cooling rate determination. It is design to eexamine quenching fluids with agitation, using the Tensi agitation apparatus [7]. Very accurate experimental data are provided by standard which are used by author of current paper to study mechanism of surface polymeric layer formation. As a liquid quenchant is used Poly(Alkylene) Glycol (PAG) inverse solubility polymer that creates stable polymeric surface layer during quenching. The proposed method explores standard cylindrical probe 12.5 mm in diameter and 80 mm long and is made of Inconel 600 material [1, 6]. Thermal diffusivity and thermal conductivity of Inconel 600 material versus temperature are provided in Table 1.

Table 1: Thermal diffusiyit and thermal conductiyit of Inconel 600 material versus temp erature.

T, °C	$a \cdot 10^{-6} m^2/s$	$\bar{a} \cdot 10^{-6} m^2/s$	$\lambda, W/m^2K$	$\bar{\lambda}, W/m^2K$
100	3.7	3.7	14.2	14.2
200	4.1	3.9	16	15.1
300	4.5	4.1	17.8	16
400	4.8	4.28	19.7	17
500	5.1	4.44	21.7	17.8
600	5.4	4.6	23.7	18.8
700	5.6	4.74	25.9	20
800	5.8	4.88	26.3	20.06
900	6.0	5	28	21

Fig. 1 present accurate experimental cooling curves and cooling rates for Inconel 600 standard probe 12.5 mm diameter. These accurate experiments are used to see how dimensionless number Kn changes versus time. The aim of such recalculations is to get knowledge on polymeric surface layer behavior during quenching.

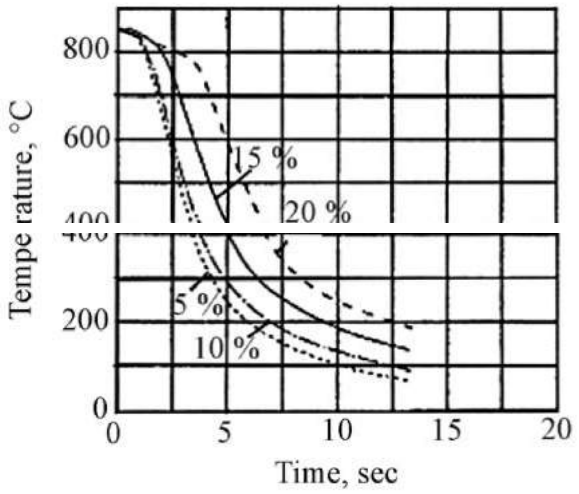

a)

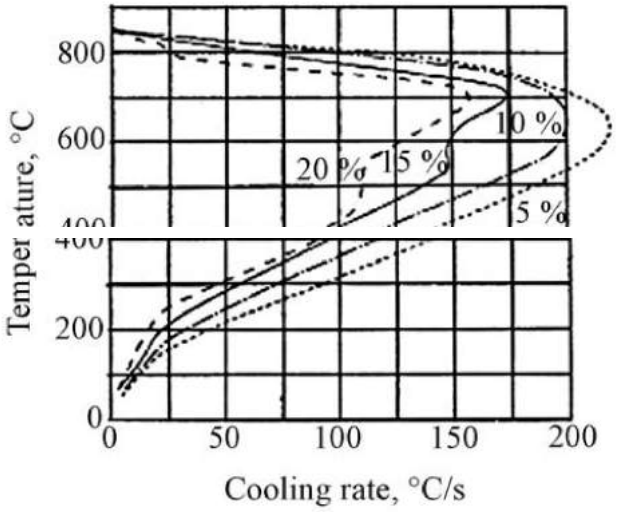

b)

Fig. 1: Illustration of the effect of quenchant concentration on cooling curve performance for PAG solutions at 30 °C and agitation 0.5 m/s [7]: *a* – cooling curves versus time; *b* – cooling rate versus time

As well known, presented cooling characteristics allow comparing experiments between each other and cannot be used directly to calculate cooling time and cooling rate the real steel parts during quenching. The goal of investigation is establishing correlation between standard Inconel 600 probe and real steel parts of different sizes and forms to have mathematical tool for recipes development. As known cooling rate of any form of steel parts is calculated as [1, 8]:

$$v = \frac{a\,Kn}{K}\left(T - T_m\right) \tag{1}$$

or

$$Kn = \frac{vK}{a\left(T - T_m\right)} \tag{2}$$

$$Kn = \Psi \cdot Bi_V \tag{3}$$

$$\Psi = \frac{\overline{T}_{sf} - T_m}{\overline{T}_V - T_m} = \frac{1}{\left(Bi_V^{\,2} + 1.437\,Bi_V + 1\right)^{0.5}} \tag{4}$$

Here v is core cooling rate of steel part during quenching in °C/s; a is thermal diffusivity of material in m²/s; Kn is dimensionless Kondrat'ev number; K is Kondrat'ev form factor

in m²; T_m is bath temperature; Bi_V is generalized Biot number; $\overline{T}_{sf}$ is average surface temperature; $\overline{T}_V$ is average volume temperature; Ψ is non-smoothness temperature in steel part.

Note that dimensionless number Kn varies within $0 \le Kn \le 1$ (see Table 2) and can adequately indicate intensity of cooling. When Kn = 1, cooling is ideal and depends only on thermal diffusivity of material and form and size of steel parts. This condition is called $Bi_V \to \infty$

Table 2: Kondrat'ev number Kn versus generalized Biot number Bi_V [8].

Bi_V	Ψ	Kn	Bi_V	Ψ	Kn
0.00	1	0.00	6	0.14	0.888
0.1	0.93	0.093	7	0.129	0.903
0.2	0.87	0.174	8	0.114	0.915
0.4	0.76	0.304	9	0.103	0.924
0.6	0.67	0.402	10	0.093	0.931
0.8	0.60	0.479	15	0.064	0.953
1	0.54	0.539	20	0.048	0.965
2	0.36	0.713	30	0.033	0.976
3	0.264	0.793	40	0.025	0.982
4	0.21	0.839	50	0.018	0.096
5	0.174	0.868	100	0.010	0.99
5.5	0.16	0.879	∞	0	1

To see physical meaning of dimensionless number Kn, let's analyze experimental data received during quenching in 5% water solution NaOH which was tested by French [9]. This solution provides extremely fast cooling and tends to ideal condition (see Fig. 2 and Fig. 3).

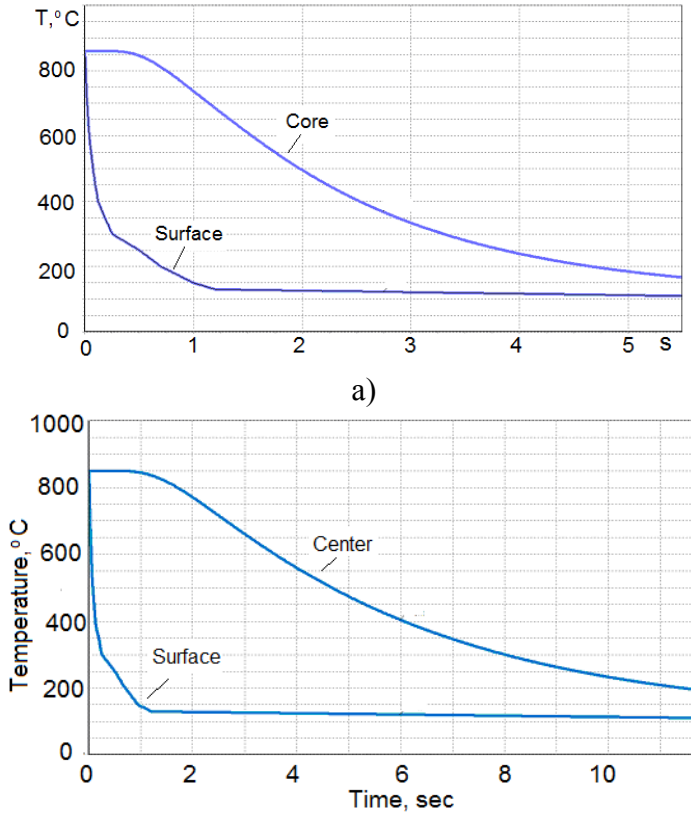

Fig. 2: Surface and core cooling curves versus time during quenching cylindrical specimens in 5% Water solution NaOH at 20°C: a – standard probe. 12.5 mm diameter; b – cylindrical probe 20 mm.

Early scientists established three principles to be successfully used for quench process design [10].

They include possibility to explore the same surface cooling curves for different sizes and forms of steel part quenched in liquid where any film boiling is absent. Evaluation the duration of transient nucleate boiling process during quenching steel in liquid media. And possibility to evaluate surface temperature of any steel part during transient nucleate boiling.

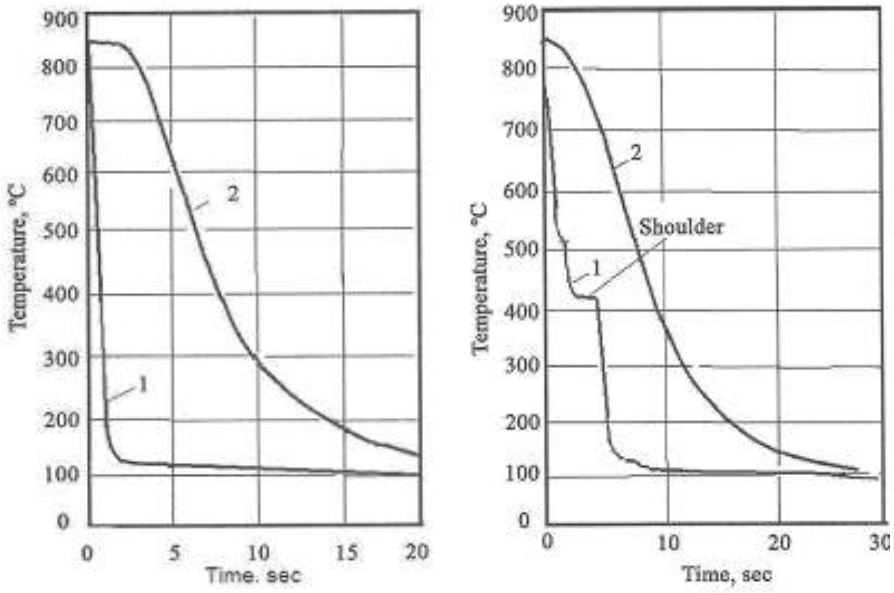

a) b)

Fig. 3: Surface and core cooling curves versus time during quenching cylindrical specimens (20 mm diameter) in low concentration (< 1%) polyoxyethylene at 20°C [11]: a – normal cooling curves; b – surface cooling curve with a shoulder formation.

All three principles are seen from Fig. 2. Surface temperature in all tests drops from 850°C to 150°C within one second independently of size of probe. Surface temperature during nucleate boiling maintains on the level of boiling point of a liquid. Duration of nucleate boiling is evaluated by established correlation on laws of quenching process [10]. It became clear that the real and effective dimensionless numbers Kn are linear function versus time (see Fig. 4) [12].

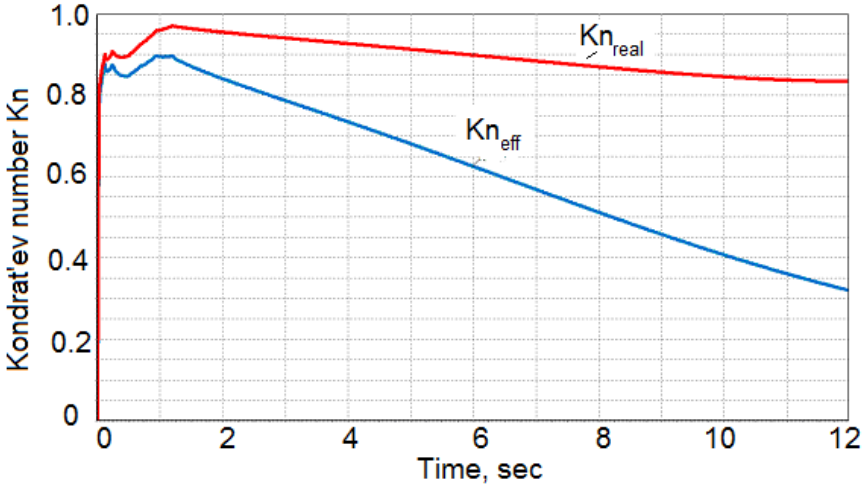

Fig. 4: Real and effective Kondrat'ev numbers versus time during quenching cylindrical specimens (20 mm diameter) in 5% water solution NaOH.

Average real dimensionless number is equal to 0.9. Average effective dimensionless number is equal to 0.65 (see Fig. 4). Real Kn number is responsible for temperature gradient formation. Effective Kn number can be used only for core cooling time and core cooling rate evaluation [1, 12].

According to the patented technology [1, 13], intense cooling process is considered when 0.8 < Kn < 1. It means that 5% water solution of NaOH solution provides intensive quenching during transient nucleate boiling process. Cooling process during convection is slow. Further these data will be used to compare them with the water PAG solutions data.

Cooling curves on Fig. 3 are similar, however, cooling process a little bit decreases due to surface polymeric layer formation that creates thermal resistance [14].

2.2 Surface polymeric layer eliminates any film boiling process

For the first time intensive quenching process during quenching in low concentration of PAG solution was observed by authors [1]. It was not clear why that is happening. Author [12] explained uniform and accelerated cooling by surface polymeric layer formation that decreases initial heat flux density below its critical value (see Fig. 5 , Fig. 6, and Eq. 5).

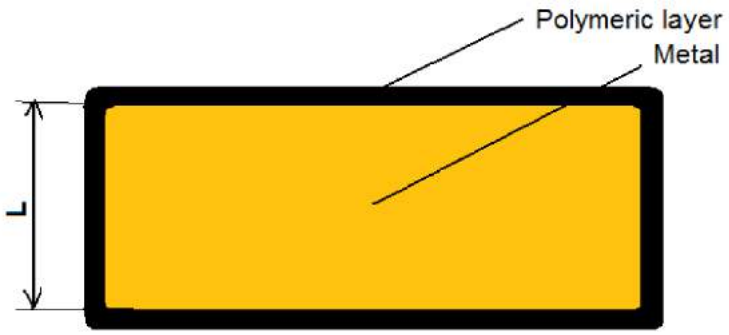

Fig. 5: Steel part covered by insulating layer.

As seen from Fig. 6, initial heat flux density during quenching in water NaOH solution is equal to 14 MW/m².

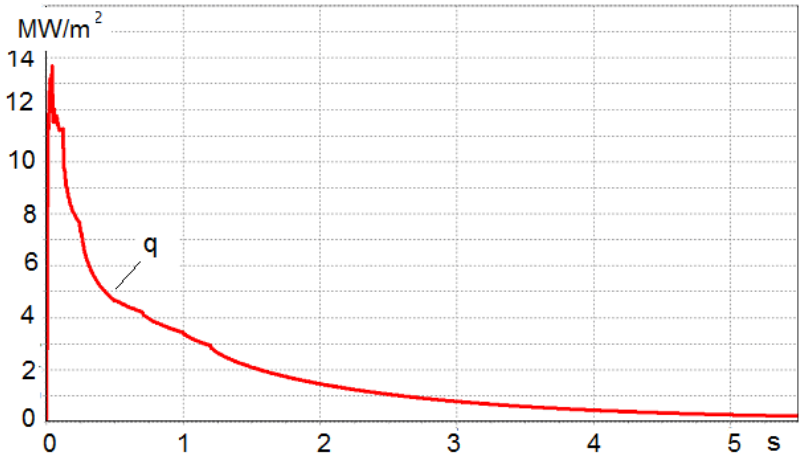

Fig. 6: Heat flux density versus time during quenching standard probe in 5% water NaOH solution.

Let see how much we can reduce it if thickness of insulating layer is 0.1 mm or 10 x 10^{-6}m. Radius of standard probe is 0.00625 m. Average thermal conductivity of Inconel 600 material is 20 W/mK while thermal conductivity of insulating layer is 0.2 W/mK. Using equation (5), calculate heat flux

density reduced by formation of insulating layer. This simple calculation show that initial heat flux density reduces from 14 MW/m² to 4.1 MW/m². According to authors [3, 4], the first critical heat flus density for water at 20°C is equal 5.8 MW/m². It means that film boiling is absent since initial heat flux density is below its critical value q_{cr1}.

$$q_{in} = \frac{q_o}{1 + 2\frac{\delta}{R} \cdot \frac{\lambda}{\lambda_{coat}}} \quad (5)$$

It was established by author [15] that during immersion probe into water PAG solution surface polymeric layer forms immediately (see Fig. 7). If film boiling is absent, polymeric surface layer is formed within 0.05 s – 0.25 s [15, 16].

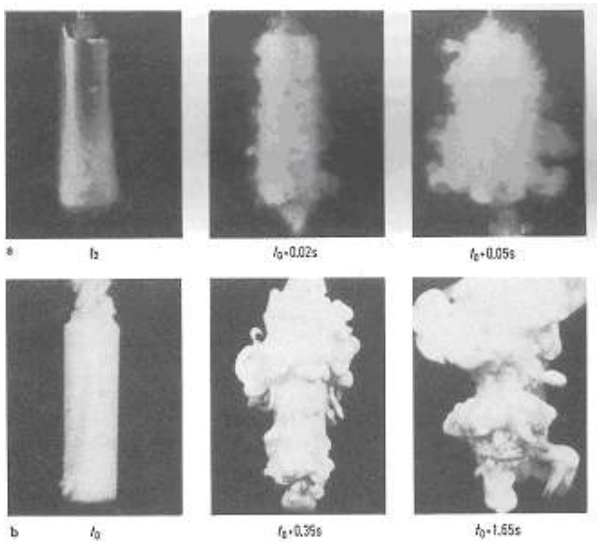

Fig. 7: Formation of surface polymeric layer during quecheing cylindrical probe 15 mm diameter in water solution of 10% of polymer at 29°C [15, 16]: a) start of polymeric layer formation 20 sec; b) start of polymeric layer formation 6 sec.

It should be noted here that currently polymeric layer is used also for the film boiling elimination during quenching in oils (see Fig. 8). Authors [17, 18] dissolved polyisobutelene (PIB) in mineral oil (3%) to provide uniform hardness, decrease distortion of hardened steel parts and decrease emission due to absence of film boiling process. Solution with 3% PIB in oil is currently used in heat treating industry [18].

Fig. 8: Polymeric surface layer formation during quenching standard probe in oil [17, 18].

New quenchant was introduced for hardening bearing rings and rollers where problem with distortion often arises [17, 18].

III. COOLING CURVES ANALYSIS TO OBSERVE VARYING THICKNESS OF SURFACE INSULATING LAYER

As known, the real heat transfer coefficient (HTC) during transient nucleate boiling process is calculated as a ratio of the heat flux density produced by bubbles to the overheat of the boundary layer [3, 5] that is a realistic indicator of temperature gradient value. Here we have to use effective Kn_{eff} as a tool for intensity process investigation because there were no enough experimental data for real Kn evaluation. For this purpose Eq. 2 was used.

As already known, the coating (insulating layer) forms immediately after immersion probe into water polymer solution. Coating starts decrease its thickness due to dissolving polymer with passing time. It means that dimensionless number Kn slightly increases because decreases thermal resistance. When insulating layer is completely dissolved and convection mode starts, dimensionless number decreases since heat transfer coefficient during convention is low and decreases with time. Detail results of calculations are presented in Fig. 9, Fig. 10, and Fig. 11.

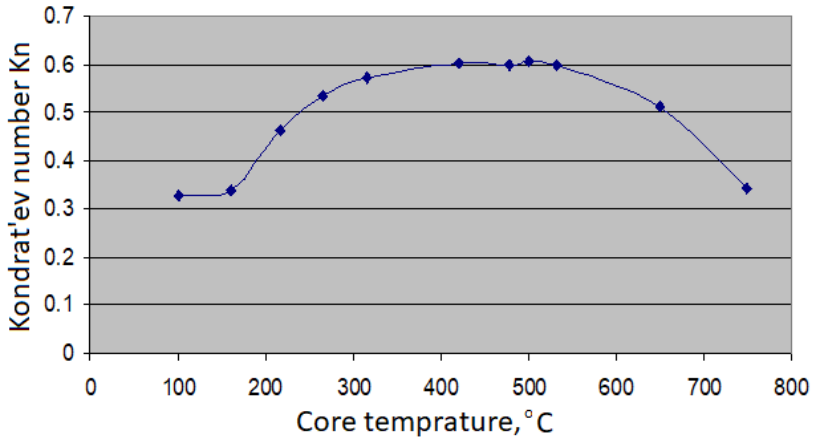

Fig. 9: Dimensionless effective number Kn versus core temperature of standard probe during its quenching in 5% PAG solution at 30°C and 0.5 m/s agitation

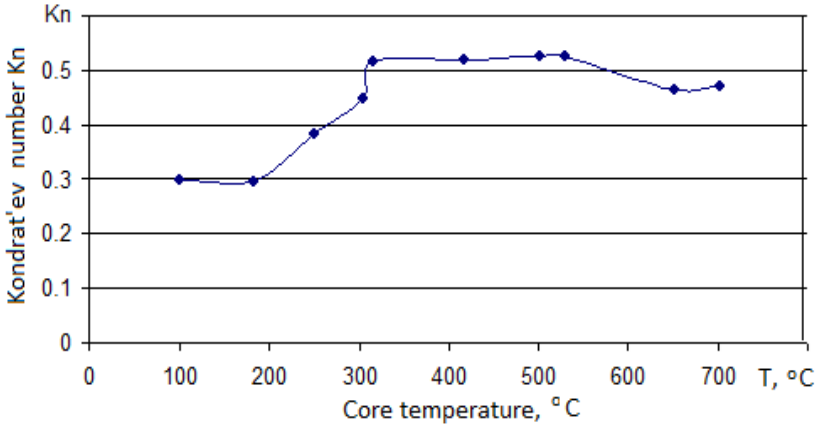

Fig. 10: Dimensionless effective number Kn versus core temperature of standard probe during its quenching in 10% PAG solution at 30°C and 0.5 m/s agitation

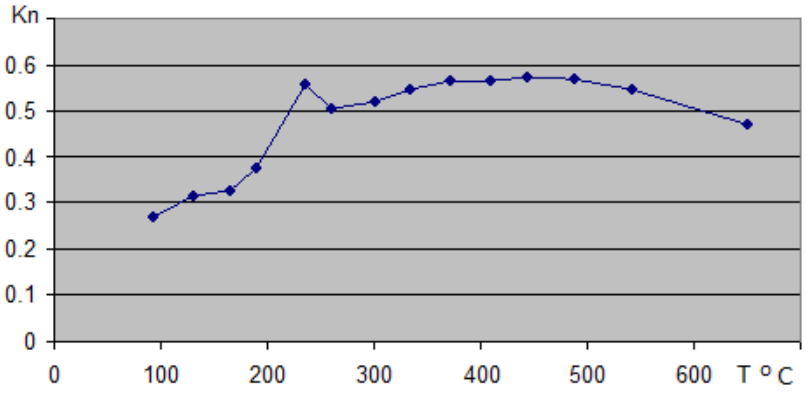

Fig. 11: Dimensionless number Kn versus core temperature of standard probe during its quenching in 3% Aqua-quench 365 water polymer solution at 38°C and moderate agitation

Comparison of dimensionless effective Kn numbers for different polymeric quenchants is provided in Table 3.

Table 3: Comparison of dimensionless effective Kn numbers for different polymeric quenchants

Quenchant	Kn	Comments
PAG , 5%	0.58	Thickness of insulating layer is not proportional
PAG, 10%	0.50	to water polymer solution
Aqua-quench 365, 5%	0.53	Differs insignificantly from PAG solution

More useful information on cooling intensity of polymer water solutions can be provided by testing Liscic probe [19]. Some results of test are shown on Fig. 12.

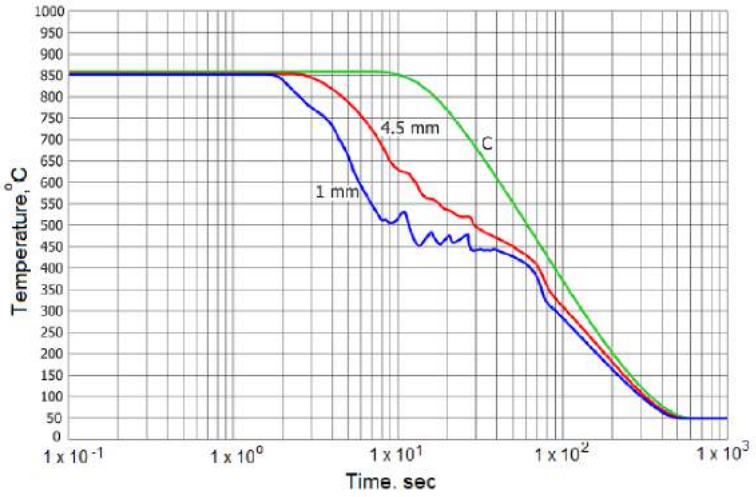

Fig. 12: Cooling curves measured by the Liscic probe (50 mm diameter) quenched in polymer solution at 35 °C, with agitation [19, 20].

On the cooling curve depicted on a distance 1 mm below surface, one can see shoulder formation reminding shelf. Further investigations in this area were fulfilled by team of scientists from Germany [21]. They tested huge shaft 150 mm in diameter and 450 mm long. Three thermocouples were welded on the surface of shaft and one thermocouple was welded on the bottom end of shaft. All three surface thermocouples showed "shoulder" formation at 350°C. Authors explained

shoulder formation by film boiling process development [21]. However, by solving inverse problem, is clear that heat transfer coefficient (HTC) at the area of shelf formation significantly prevails HTC at film boiling process. Author [22] came to conclusion that shoulder formation is caused by varying surface polymeric layer during quenching probes in water PAG solutions.

As one can see from Fig. 13, dimensionless effective number Kn_{eff} during quenching in 5% water solution of NaOH gradually decreases versus core temperature of standard probe while effective number during quenching probe in 10% water PAG solution, in contrary. increases significantly. There is no contradiction here, just almost instantly formed thick polymeric surface layer starts to dissolve by vapor bubbles. At normal atmospheric pressure diameter of vapor bubble is 2.3 mm, and release frequency is 76 Hz [3]. Number of active bubbles depend on developed heat flux density. The higher is the heat flux density, the higher are numbers of active bubbles which start to dissolve insulating layer. Mechanism of polymeric layer dissolving is caused by pumping mechanism of bubbles release. Vapor bubble push away hot water from hot boundary layer replacing it by cold water.

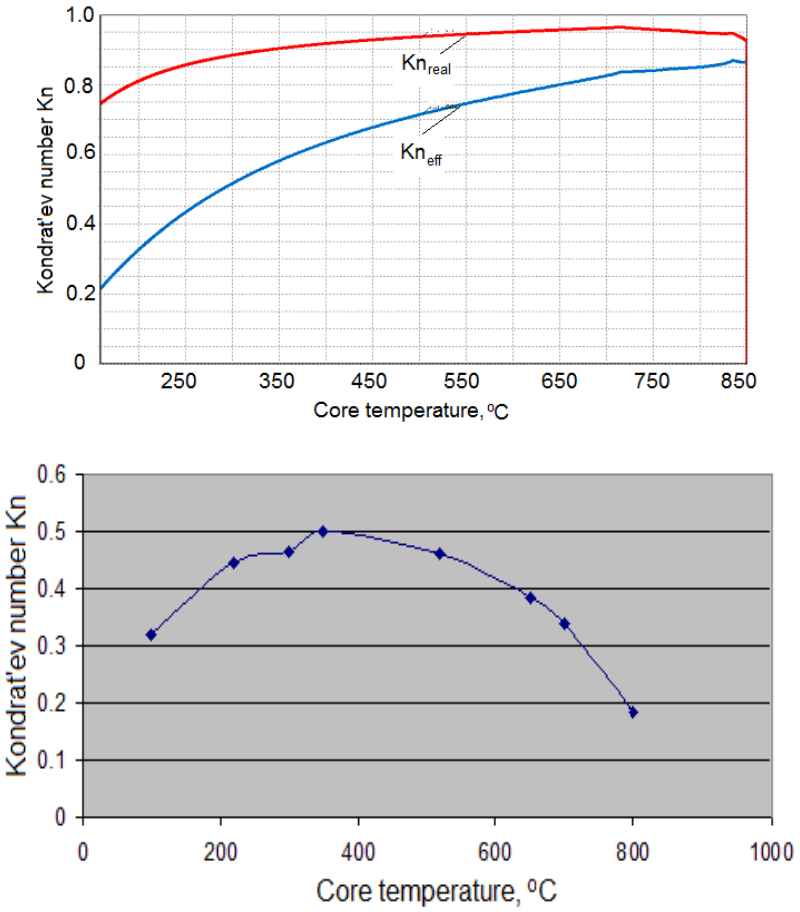

Fig. 13: Real and effective dimensionless numbers Kn versus core temperature of standard probe 12.5 mm: a – quenching in 5% solution odf NaOH; b – quenching in 10% water solution of PAG 27°C and agitation 15 L/min.

Cold water dissolves surface polymeric layer. However, heat flux density decreases with passing time resulting in decrease active bubbles which cannot more compete with depositing of surface polymeric layer. Beginning from this point of time thickness of polymeric layer gradually increases. Especially such effect is taking place when quenching in PAG polymer solutions of large steel parts.

Such simple and very interesting mechanism of dissolving surface polymeric layer is used to

explain shoulder formation on the cooling curve during quenching (see Fig. 3. b)).

IV. BENEFITS CAUSED BY OPTIMIZING INSULATED POLYMERIC SURFACE LAYER DURING QUENCHING

4.1 Optimal hardenability steel quenched in low concentration of PAG solutions

Quenching in water polymer solution of low concentration provides maximal intensity of steel parts cooling. According to accurate data of author [23], accelerated steel quenching in water polymers solutions of inverse solubility results in surface compressive residual stresses formation and superstrengthening of material. These phenomena take place when surface hardened layer is optimal or cooling is interrupted at proper time to create such hardened layer [24, 25]. Optimal hardened layer in optimal hardenbility steel (OHS) is formed if correlations (6 and 7) are true:

$$\frac{DI}{D_{opt}} \cdot Kn^{0.5} = 0.35 \pm 0.095 \quad (6)$$

$$DI = 25.4 \cdot k_{Fe} \cdot k_{Mn} \cdot k_{Si} \cdot k_{Cr} \cdot k_{Ni} \cdot k_{Mo} \ldots . \quad (7)$$

In heat treating industry is used low hardenability steel containing minimum alloy elements. Intensive quenching of low hardenability (LH) steel results in increasing service life of machine components, in saving energy and materials [26]. The LH steel can serve as an optimal hardenability steel for small gears and shafts. Its chemical composition is provided below in wt % [26]: C: 0.40 - 0.85; Mn: ≤ 0.20 ; Si: ≤ 0.20; Cr: ≤ 0.10 ; Ni: ≤ 0.10 ; Cu: ≤ 0.10 ; Al: 0.03 - 0.10; Ti: 0.06 - 0.12 ; V: ≤ 0.40 . Proposed steel chemistry is used for manufacturing small gears and shafts. Unfortunately, there is no a method for its chemistry optimizing depending on size and form of quenched samples. As the next step in optimizing quenching processes is optimal hardenability steel. It provides optimal hardened layer for any size and form of machine component and its chemical composition is (in wt, %) [24]: C: 0.30 - 1.20; Mn ≤ 0.20; Si: ≤ 0.20 ; Cr: ≤ 0.50 ; Ni: ≤ 1.6; Mo: ≤ 0.25 ; Cu: ≤ 0,20; Al: 0.03 - 0.10; Ti: 0.06 - 0.12; V: ≤ 0.40; S: ≤ 0,035; P: ≤ 0.035 . Both steels provide fine microstructure due to containing small amount of aluminum; vanadium and titanium. Proposed steel chemistry is used for manufacturing different sizes and forms machine components. There is a method for its chemistry optimizing depending on size and form of quenched samples which was tested in the practice. In contrast to LH steel, OH steel can be quenched in low concentration of water polymer solutions that significancy extends its use.

4.2 Alloy steel quenched in low concentration of PAG solutions

If alloy steel is through hardened, it develops in many cases tensile surface residual stresses after quenching. To create compression residual stresses for such steel, cooling rate should be interrupted at a temperature within interval 400°C – 500°C [1]. Let s consider an example proposed technology.

A squares plate 150 mm long and 15 mm thickness is quenched from 860°C in low concentration of water PAG solution at 30°C. Plate is made of AISI 4340 steel. It should be provided compressive residual stresses at the surface of plate after quenching. Some initial data are known. Dimensionless number Kn is equal to 0.54 (see Fig. 9). Average thermal diffusivity of steel is $5.4 \times 10^{-6} m^2 / s$. Kondrat'ev form factor K is $K = l^2 / \pi^2 = (0.015m)^2 / 9.87 = 22.8 \times 10^{-6} m^2$

Calculate core cooling time from 860°C to 300°C and provide immediate tempering of the plate at a temperature 300°C.

For cooling time calculation generalized equation (8) is used [1]:

$$\tau = \left[\frac{kBi_V}{2.095 + 3.867 Bi_V} + \ln \frac{T_o - T_m}{T - T_m} \right] \cdot \frac{K}{aKn} \quad (8)$$

Knowing Kn it is possible to get generalized Biot numberBi$_V$ from Table 3 which is equal 1. According to Eq. (8), duration of quenching in water polymer solution is:

$$\tau = \left[\frac{2 \times 1}{2.095 + 3.867 \times 1} + \ln\frac{860^{o}C - 30^{o}C}{300 - 30^{o}C}\right] \cdot \frac{22.8 \times 10^{-6} m^{2}}{5.4 \times 10^{-6} m^{2} / s \times 0.54} = 11.4 \sec$$

For water polymer solution of normal and elevated concentration, dimensionless numbers Kn can be used from Fig. 14.

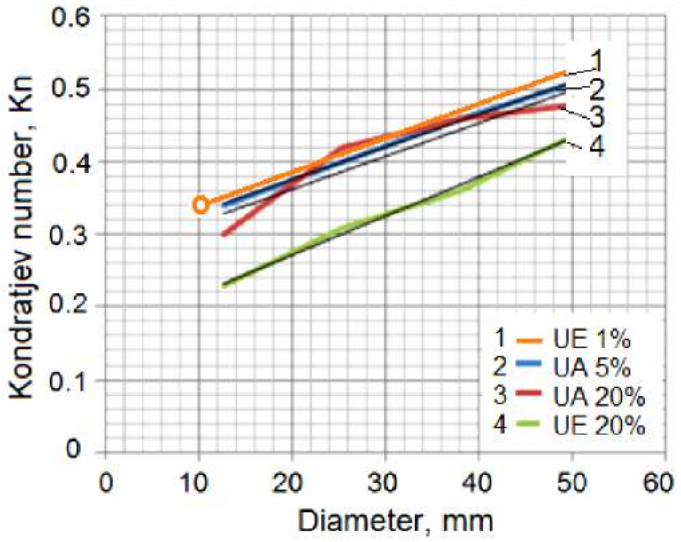

Fig. 14: Dimensionless number Kn versus diameter of tested probes during quenching in PAG solutions at 38°C [23].

4.3 High and low temperature mechanical treatment

The installation shown on Fig. 15, was discussed in literature [1]. This time, there is an opportunity for combining two effects together: increase the first critical heat flux density of liquid and decrease initial heat flux density of quenched steel part. This combination creates uniform and intensive quenching since film boiling cannot appear at all. To be more specific, let's quench a plate. The plate (L_1 = 20 mm; L_2 = 60 mm; L_3 = 80 mm) after forging with intensity of deformation 35% is quenched in low concentration (3%) of PAG water solution under pressure 0.3 MPa. Quenchant saturation temperature is 134°C. Martensite starts temperature for high carbon steel U12A is 130°C. Kondrat'ev form factor K for plate is

$$K = \frac{1}{\pi^{2}\left(\frac{1}{L_1^2} + \frac{1}{L_2^2} + \frac{1}{L_3^2}\right)}$$ [1]. Average thermal diffusivity of steel is $a = 5.4 \times 10^{-6} m^{2}$; Dimensionless number Kn = 0.54. Taking all into account, core cooling time was calculated for interval of temperatures: from 900°C to 600°C which is equal 28 sec. So, specimen was quenched in the installation (see Fig. 15) under pressure 0.3 MPa for 28 seconds and then forged again to form cutting tool and put into liquid nitrogen for 30 minutes for deep cold treatment. The technology allowed using plain carbon steel instead of alloy high carbon steel and increases service life of cutting tool. High and low temperature thermomechanical treatment (further we'll call it mechanical treatment) was investigated by many leading researchers [27, 28, and 29]. Thermomechanical treatment was used mainly for condition of slow cooling that

significantly decreases strengthening effect. This issue was discussed by authors [30, 31]. It has been shown by authors [31] that thermomechanical treatment combined with accelerated quenching further increases mechanical properties of material. Also promising idea is combining the surface martensitic microstructure with the fine bainitic microstructure at the core of quenched steel parts [32, 33].

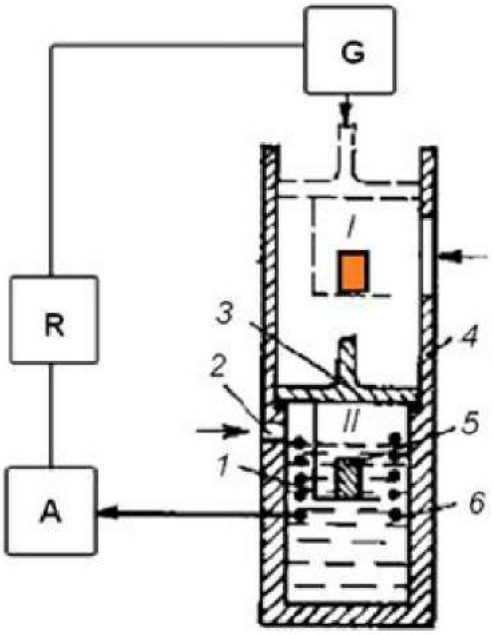

Fig. 15: Basic scheme of the automated process of steel quenching in water and aqueous solutions under pressure [1]: 1, tray; 2, aperture for pumping in compressed air; 3, mobile piston (cover); 4, case of the quench tank; 5, the part to be quenched; 6, solenoid for fixing the initial time of transformation of austenite into martensite; A, the amplifier of a signal of the martensite start; R, relay of current; G, driving mechanism; I, starting position; II, work position.

The considered process is shown schematically on Fig. 16.

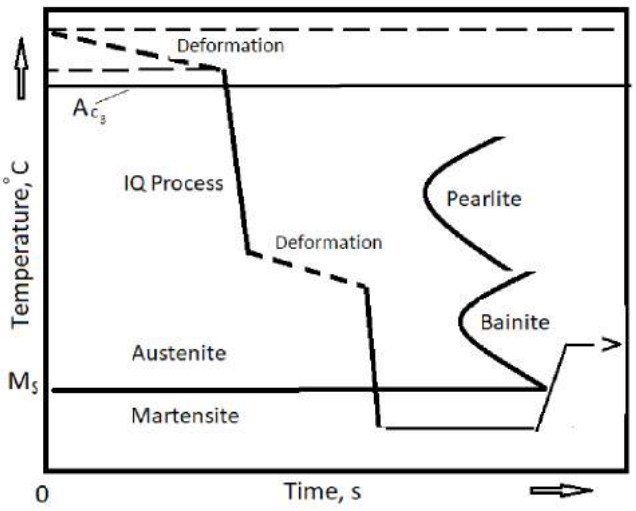

Fig. 16: High and low temperature mechanical treatment (Scheme).

Some experimental results on strength material improvement are collected in Table 4.

Table 4: Mechanical properties of steel 30KhN2MA after normal, high temperature (HTMT) and low temperature (LTMT) mechanical treatment [1, 24, and 25].

Technology	In Water			In Oil		
	R_m	Z,%	A.%	R_m	Z,%	A.%
Normal	1864	8.3	5.3	1777	10	7
HTMT	2007	9.8	5.7	919	9.9	6.3
LTMT	2600	9.2	5.7	1716	10.4	7.4

One can expect that combining thermomechanical treatment with the accelerated quenching in PAG water solutions will result in essential strength improvement of materials. That belief is based on comparison cooling rates of standard probes (see Table 5).

Table 5: Cooling rate at the core of standard cylindrical probes vs temperature and condition of cooling

Quenchant	Cooling rate in °C/s		
	300°C	500°C	700°C
Oil	30	56	85
PAG, 5%	95	187	205

As seen from Table 5, water solutions of polymers cool center of probes almost three times faster and uniformly when film boiling is completely absent. More information on cooling intensity of PAG quenchants is available in published papers [34, 35].

V. DISCUSSION

The main target of current paper is mechanism of formation and dissolving the surface polymeric layer which makes possible to understand how one can effectively eliminate film boiling process during quenching. A shoulder formation on the surface cooling curve also is a goal. These two issues are very important for introducing new technologies into practice. If any film boiling during quenching in liquid media is completely absent, cooling process is uniform and, in many cases, intensive. Mechanism of shoulder formation and understanding its physics makes more believers. A possibility to perform austempering process via cold water polymer solutions can bring big benefits for heat treating industry.. Currently, for this purpose melted salts and alkalis are used that harm environment. However, further painstaking experiments in this pass are needed which include:

- More detail investigation the mechanism of surface polymeric layer formation.
- Evaluation thermal properties of insulating layer and its thickness variation.
- Elaboration of special additives to increase the first critical heat flux density.
- Establishing correlation between thickness of insulating layer and the thickness of quenched steel parts to guarantee absence film boiling process during quenching.
- Studies on stability of shoulder formation and evaluating temperatures at which phenomenon takes place.
- Optimization the cooling processes taking place during quenching steel covered by insulating layer.
- Mathematical description of quenching processes to make automation possible.

Such investigations will make environment green, improve strength of material and decrease their cost.

VI. CONCLUSIONS

An insulating polymeric layer formed during quenching in inverse solubility polymers is used to shift initial heat flux density below its critical value. This shifting eliminates any film boiling process that provides uniform cooling, decreases

distortion, increases strength of material and improves environment condition.

Optimized cooling process during hardening materials in inverse solubility polymers in the interval of transient nucleate boiling temperatures is intensive since dimensionless Kondrat'ev number Kn is within 0.8 < Kn < 1 and slow cooling during convection.

Basics of performing hardening materials in optimal concentration of inverse solubility polymers is proposed to make appropriate calculations and design software and automate technological processes.

It is expected that, due to surface insulating surface layer, low and high temperature mechanical treatment will result in increasing service life of machine components and tools.

Two the most promising directions: study of critical heat flux densities and behavior and mechanism of surface insulating layer formation should be carefully further investigated since they'll bring essential benefits for heat treating industry.

REFERENCES

1. Kobasko N.I., Aronov M.A., Powell J.A., and Totten G.E., Intensive Quenching Systems: Engineering and Design, ASTM International, W. Conshohocken, PA, USA, 2010, 234 p.
2. Kobasko N.I. Contemporary Methods of Steel Hardening in Liquid Media Based on Laws of Modern Physics, *Research & Reviews: Journal of Pure and Applied Physics (RRJPAP),* Vol. 9, Issue 5, March 2021, pp. 6 – 17.
3. Tolubinsky V.I.. Heat Transfer at Boiling. Kyiv: Naukova Dumka, 1980.
4. Kutateladze, S. S.Fundamentals of Heat Transfer, Academic Press, New York, 1963.
5. Kobasko N, *Austempering processes that are performed via cold liquids,* Lambert Academic Publishing, Germany, 2019, 84 p.
6. Totten G.E., Bates C.E., and Clinton N.A. *Handbook of Quenchants and Quenching Technology*, Materials Park, ASM International, 1993, 507.
7. ASTM Standard Method: Standard Test Method D 6482 – 06 for Determination of Cooling Characteristics of Aqueous Polymer Quenchants by Cooling Curve Analysis with Agitation (Tensi Method). Annual Book of ASTM Standards, ASTM International, West Conshohocken, PA, 2000.
8. Kondrat'ev, G. M., Thermal Measurements. Moscow: Mashgiz, 1957.
9. French H.J. *The Quenching of Steels*. Cleveland, Ohio, USA: American Society for Steel Treating, 1930.
10. Kobasko N.I., Basics of quench process hardening of powder materials and irons in liquid media, *European Journal of Applied Physics,* Vol. 4, No. 3, 2022, pp. 30 – 37.
11. Kobasko N, *High Quality Steel vs Surface Polymeric Layer Formed during Quenching*, Lambert Academic Publishing, Germany, 2019 84 p.
12. Kobasko, N. I. (2012). Real and Effective Heat Transfer Coefficients (HTCs) Used for Computer Simulation of Transient Nucleate Boiling Processes during Quenching. Materials Performance and Characterization, 1 (1), MPC.– 2012–0012 doi: 10.1520/mpc-2012-0012.
13. US Patent No. 6,364,974, April 2, 2002, Quenching Apparatus and Method for Hardening Steel Parts.
14. Kobasko N., *Advanced Quenching Technologies,* Lambert Academic Publishing, Germany, 2021, 119 p.
15. Tensi H.M., Wetting Kinematics. A Handbook "Theory and Technology of Quenching." . Spriger – Verlag. Berlin. 1992. pp. 93 - 116.
16. Tensi H.M., Schwalm M., Wirkung von Abschreck Flüssigkeiten unter Berücksi chtigung spezieller wassriger Polyethy lenoxide, In: *HTM*, 35, 122 -129.
17. Logvynenko P.N., *et.al.,* Oil quenchant, UA Patent No. 104380, 2016.
18. Kobasko N., Moskalenko A., Logvinenko P. *at.,al.*, An effect of PIB additives to mineral oil resulting in elimination of film boiling during steel parts quenching. *EUREKA: Physics and Engineering*. Number 3. 2016.
19. Liščić, B. Measurement and Recording of Quenching Intensity in Workshop Conditions

Based on Temperature Gradients. Materials Performance andCharacterization, 2016, 5 (1), MPC20160007. doi: https://doi.org/10.1520/mpc20160007.
20. Kobasko N.I., Liščić, B., Liščić/Petrofer probe to investigate real industrial hardening processes and some fundamentals during quenching of steel parts in liquid media, «EUREKA: Physics and Engineering» , Number 6, 2017, pp. 48 – 55.
21. Waldeck S, Castens M, Riefler N, Frerichs F, Luebben Th, Fritsching U, et al. Mechanisms and Process Control for Quenching with Aqueous Polymer Solutions.HTM J. Heat Treatm. Mat. 2019; 74(4):1-19. DOI:10.3139/105.110387.
22. Kobasko N., Mechanism of shoulder formation during quenching steel in water polymer solutions and its practical use as a new physical phenomenon, Theoretical Physics Letters, Vol. 9, No. 12, 2021, pp. 219 – 233.
23. Kobasko N., Moskalenlo N., Dobryvechir V., Research on use of low concentration inverse solubility polymers in water for hardening. machine components and tools. *EUREKA: Physics and Engineering,* Number 2. 2018. pp. 63 – 71.
24. UA Patent 114174. C2 (2017). Alloyed low hardenability steel and method for its composing. Filled on September 23. 2013. File number a 201311311.
25. Kobasko, N., *Optimal hardenability steel and method for its composing*. Lambert Academic Publishing, 2018. 124. ISBN: 978-613-9-82531-8. RU Patent № 2158320, 1999.
26. Bernshtein M.L. Thermomechanical Treatment of Metals and Alloys, Metallurgiya, Moscow, Vol. I. 1968;1:586.
27. Bernshtein M.L. Thermomechanical Treatment of Metals and Alloys, Metallurgiya, Moscow, Vol. II. 1968;2:575.
28. Tamura C., Ouchi T., et. al. Thermomechanical Processing of High Strength Low Alloy Steels, Butterworths, London, 1988.
29. Kobasko N.I. Thermal and Metallurgical Basics of Design of High-Strength Steels, In a Book "Intensive Quenching Systems: Engineering and Design", N.I.Kobasko, M.A. Aronov, J.A.Powell, G.E.Totten (Eds.), ASTM International. W.Conshohocken, USA, 2010, pp. 1–23.
30. Aronov M.A. & Powell J.A. Forging Process Improvement Using Intensive Quenching Immediately After Forging Operationsare Completed. Proceedings of the Forging Industry Association Technical Conference, Columbus, Ohio, USA, 2016.
31. Grossmann M.A., *Principles of Heat Treatment*, American Society for Metals, Ohio, USA, 1964, 303 p.
32. Bhadeshia, H. K. D. H. (2015). Bainite in Steels: Theory and Practice (3rd edition), Money Publishing, 616.
33. Kobasko, N. (2021). Cooling process optimization during hardening steel in water polyalkylene glycol solutions. *Technology Audit and Production Reserves*, 6 (1 (62)), 27–35. doi: https://doi.org/10.15587/2706-5448.2021.247736.
34. Moskalenko, A. A., Kobasko, N. I., Tolmacheva, O. V., Totten, G. E., Webster, G. M. (1996). Quenchants characterization by acoustical noise analysis of cooling properties of aqueous poly (alkylene glycol) polymer quenchants. 2-nd International Conference on quenching and Control of the Distortion.
35. Lohvynenko, P. N., Moskalenko, A. A., Kobasko, N. I., Karsim, L. O., Riabov, S. V. (2016). Experimental Investigation of Effect of Polyisobutilene Additives to Mineral Oil on Cooling Characteristics. Materials Performance and Characterization, 5 (1), 1–13.

Genetic Characterization and Evolution of Populations of *Helicoverpa Amigera* (Lepidoptera Noctuidae) Subservient to the Various Host Plants in the Niayes Zone (Senegal)

Ousmane Kébé, Adja Ndiaya Ndoye Ndiaye, Mama Racky Ndiaye, Mamadou LO, Toffène Diome, Cheikh Thiaw & Mbacké Sembène

Cheikh Anta Diop University

ABSTRACT

In Senegal, market gardening is one of the most important sectors. It makes it possible to reduce youth unemployment. However, vegetable farming faces several abiotic and biotic problems such as insect pests. The lepidopteran Noctuidae Helicoverpa armigera is one of the most formidable. This study aims to genetically characterize populations of Helicoverpa armigera on its host plants in the Niayes area using the cytochrome oxidase I (COI) gene to see if the host plants have an effect on the genetic structuring of insect populations. Genetic analyses have shown a great haplotypic diversity between the different host plants. A lack of genetic differentiation was also noted between the populations of the different host plants. Similarly, a lack of genetic structuring between the populations of the different host plants (B. oleracea, S. lycopersicum and C. annuum) was noted by a small percentage of variation between the host plants. Demogenetic tests indicate the hypothesis of an expanding population and this hypothesis is confirmed by the sum of the squares of the deviations (SSD) and the irregularity index (Rag) of the populations of H. armigera.

Keywords: helicoverpa armigera, host plants, genetic structuring, niayes zone, cytochrome oxidase i..

Classification: DDC Code: 576.58 LCC Code: QH455

Language: English

London Journals Press

LJP Copyright ID: 925692
Print ISSN: 2631-8490
Online ISSN: 2631-8504

London Journal of Research in Science: Natural and Formal

Volume 22 | Issue 6 | Compilation 1.0

Genetic Characterization and Evolution of Populations of *Helicoverpa Amigera* (Lepidoptera Noctuidae) Subservient to the Various Host Plants in the Niayes Zone (Senegal)

Ousmane Kébé[α], Adja Ndiaya Ndoye Ndiaye[σ], Mama Racky Ndiaye[ρ], Mamadou LO[ᘐ], Toffène Diome[¥], Cheikh Thiaw[§] & Mbacké Sembène[χ]

ABSTRACT

In Senegal, market gardening is one of the most important sectors. It makes it possible to reduce youth unemployment. However, vegetable farming faces several abiotic and biotic problems such as insect pests. The lepidopteran Noctuidae Helicoverpa armigera is one of the most formidable. This study aims to genetically characterize populations of Helicoverpa armigera on its host plants in the Niayes area using the cytochrome oxidase I (COI) gene to see if the host plants have an effect on the genetic structuring of insect populations. Genetic analyses have shown a great haplotypic diversity between the different host plants. A lack of genetic differentiation was also noted between the populations of the different host plants. Similarly, a lack of genetic structuring between the populations of the different host plants (B. oleracea, S. lycopersicum and C. annuum) was noted by a small percentage of variation between the host plants. Demogenetic tests indicate the hypothesis of an expanding population and this hypothesis is confirmed by the sum of the squares of the deviations (SSD) and the irregularity index (Rag) of the populations of H. armigera.

Keywords: *helicoverpa armigera*, host plants, genetic structuring, niayes zone, cytochrome oxidase i.

Author α σ ρ ᘐ ¥: Genetics and Population Management Team, Department of Animal Biology, Faculty of Science and Technology, Cheikh Anta Diop University, Dakar, Senegal.

§: UFR Agronomic Sciences, Livestock, Fisheries-Aquaculture and Nutrition (SAEPAN) University of Sine Saloum El-hadji Ibrahima Niass (USSEIN) Sing-Sing, BP 55, Kaolack, Senegal.

χ: Team of Genetics and Population Management, Department of Animal Biology, Faculty of Science and Technology, Cheikh Anta Diop University, Dakar, Senegal.

I. INTRODUCTION

Agriculture is one of the main sectors of activity that contributes to the socio-economic development of populations. It produces most of the basic foodstuffs, improves the livelihoods and incomes of families. In this sector, market gardening occupies a very important place and contributes significantly to food sovereignty [27], to the fight against poverty and family incomes [26, 55]. In West Africa, market gardening is a promising driver of economic growth, a vital source of income for resource-poor producers in rural and peri-urban areas [32]. In Senegal, market gardening is one of the most important sectors. It contributes to the endemic reduction of youth unemployment [45]. However, market gardening faces several abiotic problems (the availability and quality of water for irrigation, hydro-agricultural developments, the low level of technicality as well as the lack of experience of some producers, the lack of qualified supervision, the availability of inputs) and biotic problems such as insects, nematodes and fungi [12, 28]. Many pests have been encountered on vegetable crops. They attack different crops and cause various damages to different parts of the plant [54, 21]. Thus, we were interested in *Helicoverpa armigera*, commonly known as the gram moth or fruit borer, which is a

London Journal of Research in Science: Natural and Formal

very polyphagous pest whose caterpillars are known to feed on more than 180 host plants belonging to at least 68 plant families [8]. This insect has a large migration capacity of up to 2000 km [5]. Its pupae can enter optional diapause under adverse environmental conditions such as extremely high or low temperatures [17]. With high fecundity and low generation time, capable of generating up to 10 to 11 generations per year [17], *Helicoverpa armigera* is a cosmopolitan pest, which attacks a wide range of hosts: a number of cereal crops (maize, sorghum), legumes such as groundnuts and vegetable crops such as tomatoes (*Solanum lycopersicum* L), cabbage (*Brassica oleracea* L.var capitata), pepper (*Capsicum annuum* L) etc. [12, 19, 37]. The gram moth, *Helicoverpa armigera* (Hubner) is a very formidable insect that colonizes two agro-ecosystems in an asynchronous place [37] and affects the quality and quantity of these crops, source of many economic losses and reduced yield [41, 9, 49]. Its caterpillars can cause very significant damage of up to 85% in Senegal [6], 36% in Nigeria [31]. Thus the management of *H. armigera* has become increasingly difficult due to its high reproductive potential and damage. This is the subject of the highlighting of several methods of struggle by a number of authors in order to eradicate the threats of *H. armigera*. Studies on biology [24, 42], on molecular identification [3], characterization of the mitochondrial DNA COI of *Helicoverpa armigera* [1, 38, 2] etc. have been carried out. However, in Senegal, entomological studies have been carried out in this insect but not genetic studies; hence the importance of our study.

The general objective of this study is to know the genetic diversity and structure of the populations of *Helicoverpa armigera*, a pest of vegetable crops in the Niayes area of Senegal. From this general objective, specific objectives are:

- To determine the genetic diversity of the populations of *Helicoverpa armigera* subservient to the various host plants in the Niayes area (Senegal);
- Characterize the genetic structuring of *Helicoverpa armigera* populations according to these different host plants (*Brassica oleracea, Solanum lycopersicum and Capsicum annuum*).

II. MATERIALS AND METHODS

2.1 Presentation of the study area

This study was carried out in the Niayes area which extends over a length of 180 km bordering the maritime fringe of the North of the country from Dakar to Saint-Louis via the western edge of Thiès and Louga. Its width varies from 05 to 30 km inland [13]. The Niayes are characterized by the alternation of two seasons: a wet season concentrated on three months (July, August and September) and a dry season that lasts the other nine months and during which two cycles of vegetable crops follow one another. A first cycle, from September to January and a second from February to May [12]. The hot and dry climate is characterized by the monsoon that blows during the wet season. Rainfall is low and rarely exceeds 450 mm/year. Temperatures are moderated by the circulation of the sea trade wind and strongly influenced by the cold currents of the Azores [15]. The warmest average monthly temperature hovers around 28°C. Between May and June, the presence of harmattan can raise the temperature to a maximum of 31°C [11].

2.2 Sampling

Our study population consists of a set of individuals from the same host plant. This study was carried out in different localities of the Niayes zone in Senegal: Gorom (Latitude: 14.793060 / Longitude: -17.172220), Keur Abdou Ndoye (Latitude: 14.88762 / Longitude: -17.132322), Malika (Latitude: 14.801484 / Longitude: -17.3376), Mboro (Latitude 15.135985 / Longitude: -16.881218) and Pout (Latitude: 14.771693 / Longitude: -17.059434). In each of these five localities, a significant number of caterpillars of *H. armigera* was taken at random from cabbage (*Brassica oleracea*), tomato (*Solanum lycopersicum*), pepper (*Capsicum annuum*) and lettuce (*Lactuca sativa*). The samples obtained on each host plant are put in a tube containing 95°C alcohol. These samples are coded according to two criteria: the first letter of

the genus name in uppercase and the first letter of the name of the species in lower case correspond to the species studied (*Helicoverpa armigera*) and the first letter of the name of the host plant in lower case. Example: samples of *H. armigera* taken from tomatoes are coded by Hat, those taken from cabbage are coded by Hac, those taken from pepper are coded by Hap and finally those taken from lettuce are coded by Hal. These samples obtained are brought back to the laboratory and put in a refrigerator for good preservation.

Table I: Summary table of sampling

Host plants	Sampling codes	Number of individuals sampled
Brassica oleracea	Hac	13
Solanum lycopersicum	Hat	13
Capsicum annuum	Hap	13
Lactuca sativa	Hal	8
Total	4	47

2.3 Genetic study

2.3.1. Helicoverpa armigera genomic DNA extraction

The total DNA of the insects was extracted using the Zymo research tissue protocol. To do this, each caterpillar was placed in a 1.5ml tube in which 95 µl of water and 95 µl of solid Tissue Buffer (Blue) were added for tissue dissociation and cell individualization and then 20 µl of proteinase K was added to degrade all proteins after incubation at 55 ° C throughout the night. The mixture was centrifuged at 12000 rpm for 1 minute to remove tissue debris and recover the supernatant in a new eppendorf tube. 400µl of Genomic Bending Buffer were added to this mixture and then vigorously vortexed. The mixture was then transferred to a Zymo-Spin column previously placed in a collector tube and centrifuged at 12000 rpm for 1 minute. The collector tube was discarded and the Zymo-Spin column was placed in a new collector tube. The DNA, fixed on the column, was then purified to remove any trace of contaminants and to do this, 2 washing pads, capable of passing through the silica membrane after centrifugation, were successively used. First 400 µl of DNA Pre-Wash Buffer were deposited on the Zymo-Spin column and the mixture was centrifuged at 12000 rpm for 1 minute followed by the addition of 700 µl of g-DNA Wash Buffer on the Zymo-Spin column and centrifuged at 12000 rpm for 1 minute. The column was then placed in an eppendorf tube and 50 µl of DNA Elution Buffer was then added directly to the membrane to increase the yield by 15 to 20%. The mixture was then incubated at room temperature for 5 minutes and then centrifuged at 12000 rpm for 1 minute. The DNA thus extracted was stored at -20°C.

2.3.2. Electrophoretic migratio

Preparation and deposition of samples electrophoresis consists of separating DNA fragments according to their size by migration into a solid matrix called agarose gel subjected to an electric field. The DNA molecule with a negative charge will migrate under the effect of the electrostatic field to the anode. The distance travelled, measured from the deposition wells, will depend on the size of each fragment. As a result, the larger the size of the fragment, the smaller the distance travelled and vice versa. The samples, 7µl of DNA extracts and 3µl of bromophenol blue (charge blue), will be deposited on a 1.5% agarose gel and migrated at 100 volts for 35 minutes. The migrated DNA is revealed in a darkroom under UV after passing through a bath of Ethidium BET Bromide. The size of the DNA is approximated using a SmartLadder 200bp size marker. The gel is prepared with 1.5 grams of agarose that is added to 100 ml of 0.5X TAE solution.

2. 3.3. PCR of cytochrome oxidase I.

2. 3.3.1. Gene choice: Cytochrome oxidase I

Cytochrome oxidase I (COI) is a mitochondrial gene encoding one of the three subunits of cytochrome c oxidase, a transmembrane oxidoreductase enzyme. It is the last to intervene in the mitochondrial respiratory chain. Its length is about 1540 bp [46, 30, 51, 43] in insects; it is widely used in phylogeny and phylogeography. This marker plays a very important role in the

barcoding process [10, 33]. Indeed, it is the standard fragment of the genome chosen (at least for the animal kingdom) as a genetic marker for species discrimination and to reveal cryptic diversity [23, 10]. Indeed, its rate of molecular evolution is fast enough to allow the substantial accumulation of mutations (often neutral) and therefore the discrimination not only of very closely related species (twin species) and subspecies, but also the detection of phylogeographic signal within the same species or ecologically differentiated populations (ecotypes) [7, 52, 53, 10]. As a result, it is very decisive in phylogeographic studies [4].

2.3.3.2. Amplification

The amplification was carried out in a reaction volume of 25 µl containing for some samples 2 µl of concentrated DNA and for others 3 µl of concentrated DNA with respectively 18,3 µl and 17,3 µl of ultrapure water. For the other constituents, the same volumes were used in both cases namely 2.5 µl of buffer (10x), 1µl of additional $MgCl_2$, 0.2 µl of Taq polymerase, 0.5 µl of dNTP and 0.25 µl of each primer which are 5'GGATCACCTGATATAGCATTCCC3' and 5'CCAGGTAAAATTAAATATAAACTTC3'. It is made by the repetition of cycles which ensures a multiplication by 2 of the target DNA at each cycle.

PCR is performed using the Eppendhorf thermocycler under the following conditions:

- Preliminary denaturation at 94°C for 3 minutes;
- Followed by a repetition of 35 cycles of initial denaturation at 94 °C for 1 minute; hybridization characterized by the attachment of the primers at 48 °C for 1 minute and elongation of the complementary strands at 72 °C for 1 minute;
- Followed by a final extension phase at 72°C for 10 minutes.

The PCR was completed by a hold at 10 °C for the preservation of the product by the thermocycler. An electrophoretic migration on agarose gel was also performed in order to see if the primers have clung.

2.3.4. Cytochrome Oxidase I Sequencing

Reactions were performed in a MJ Research PTC-225 Peltier thermocycler with ABIPRISM BigDye TM Terminator Cycle kits. Each sample was sequenced using the sense primer. The fluorescent fragments were purified with the BigDye Xterminator purification protocol. The samples were suspended in distilled water and subjected to electrophoresis in ABI 3730xl sequencer (Appled Biosystems).

2.3.5. Genetic Analyses

The sequences were manually corrected and aligned using the Clustal-W algorithm [50] with the BioEdit 5.0.6 software [22]. They have been thoroughly checked, cleaned and aligned to determine the homology of the sites and to be able to perform other phylogenetic analyses including the determination of genetic diversity, genetic differentiation parameters, mutation rates and demogenetic tests. However, after corrections and sequence alignments, we obtained two individuals from lettuce (*Lactuca sativa*) and we eliminated these two individuals because the number of samples from lettuce is too small and can influence genetic structuring since these two individuals can bias sampling.

2.3.5.1. Genetic Diversity

The parameters of genetic diversity including the number of polymorphic sites, the total number of mutations, the average number of nucleotide differences, the nature of the mutations (% of transitions and transversions) as well as the haplotypic and nucleotide diversities for each of our study populations were obtained using the DnaSP software version 5.10 [29] and MEGA 5 version v7.0.14 [48].

2.3.5.2. Genetic Differentiation and Structuring

The estimation of genetic differentiation between populations generally requires two indices: the degree of genetic differentiation (Fst) and the genetic distance of Nei [34]. The differentiation index (Fst) was evaluated by Harlequin software version 3.5.1.3 [14]. According to Wright, the more Fst tends towards 1, the more genetically structured populations are between them. On the

other hand, the populations do not show allelic differences if the Fst is zero. For each value of the Fst, the P-value makes it possible to accept or reject it according to whether it is respectively significant or non-significant. Intra- and inter-population genetic distances were determined with the MEGA5 program version 7.0.14 [48]. Molecular Variance Analysis (AMOVA) was performed to determine the genetic structuring of *H. armigera* populations. The analysis of molecular variance was determined by Harlequin software version 3.5.1.3 [14].

2. 3.5.3. Genetic Evolution

Mismatch distribution analysis is the graphical representation of the distribution of genetic distances between individuals in a population. This analysis is accompanied by two indices that test the fit quality of the distribution. These indices are the SSD (sum of squares of deviations) and the Raggedness (irregularity index Rag). The demographic history was estimated using the demogenetic tests, namely the D of Tajima [47] and Fs of Fu [18] under the assumption of neutrality or constant population size. Values close to zero suggest that the population is of constant size while significantly negative or positive values suggest sudden population expansions or bottlenecks respectively. The mistmatch graphs were built with DnaSP software version 5.10 [29]. The SSD and Rag indices and demogenetic tests were obtained with the Harlequin program version 3.5.1.3 [14] and the level of significance was evaluated after 10000 coalescing simulations.

2.3.5.4. Phylogenetic Reconstruction

Phylogenetic analysis allows the suggestion of a phylogenetic tree that tries to reconstruct the history of successive divergences during evolution. The haplotype network was built by the Network software ver. 5.0.0.0 in order to identify their relationships as well as graphically explore the existence of possible associations between haplotypes. The phylogenetic reconstructions of *H. armigera* were estimated by four methods: the Neighbour-Joining method is based on the matrix of genetic distances of ecotypes (the Kimura distance 2-parameter) taken two by two to model evolutionary processes; The Maximum Parsimony method considers a tree to be optimal when its total length (number of steps needed to explain the dataset being analyzed) is minimal; The Maximum Likelihood method makes it possible to test all the stories that may have generated the current dataset analyzed and the Bayesian inference which is the process of adapting a probability model to a set of data and summarizes the result by a probability distribution on the parameters of the model and on unnoticed quantities such as predictions for new observations [20].1000000 generations were made by sampling the different parameters every 1000 generations. Generations made during the ignition period are eliminated from the analyses. So conservatively, the first 250,000 generations have been eliminated (25%) and the inferences are then made on the next 750,000 generations. The reliability of a tree is therefore reduced to the reliability of its internal branches (nodes). It is estimated using the MrBAYES ver. program. 3.2.5 [25]. The robustness of the nodes was evaluated for repetitions of 1000 bootstraps. A boostrap is only considered significant if its value is greater than or equal to 70%. The phylogenetic trees of Neighbor-Joining, maximum parsimony and maximum plausibility were built by the MEGA 5 software version 7.0.14 [48] and the Bayesian inference by Mr bayes ver. 3.1.2 [25]. The visualization of the trees was done by the program FigTree version 1.4.2 [39]. The phylogenetic trees of *H. armigera* were rooted by an individual of the species *Helicoverpa zea*.

III. RESULTS AND DISCUSSION

3. 1. Results

3.1.1. Genetic polymorphism and diversity

After alignments and corrections of the COI sequences, the dataset obtained consists of 31 sequences, 11 of which come from cabbage (*Brassica oleracea*), 12 from pepper (*Capsicum annuum*) and 8 from tomato (*Solanum lycopersicum*). The dataset comprises 31 sequences each comprising 475 sites including 82 variable or polymorphic sites, 393 invariable sites, 08 singleton sites occupying the positrons: 140; 152; 163; 270; 279; 299; 399; 402 and 74 variable

informative sites in parsimonies. The frequency of mutations (Table II) is 49.06% transition type and 50.96% transversion type with 33.25% adenine; 33.25% thymine/uracil; 16.75% cytosine and 16.75% guanine. The mutation rate R is equal to 0.86%.

Table II: Percentage of transitions and transversions

Nucleotides	A	T/U	C	G
A	-	*8,47*	*4,27*	**8,22**
T/U	*8,47*	-	**8,22**	*4,27*
C	8,47	**16,31**	-	*4,27*
G	**16,31**	*8,47*	*4,27*	-

The dataset (Table III) includes 31 haplotypes, 11 from *B. oleracea*, 12 from *C. annuum* and 08 from *S. lycopersicum*. The total number of mutations is 80 for individuals of *B. oleracea*; 71 for *C. annuum* and 60 for *S. lycopersicum*. For the species *B. oleracea*, the average number of nucleotide differences is 33,709; that of *C. annuum* is 28.409 and that of *S. lycopersicum* is 27.

Table III : Genetic Polymorphism

Population	Numbers of haplotypes	Total number of mutations, Eta	Mean number of nucleotide differences, k
Brassica oleracea	11	80	33,709
Capsicum annuum	12	71	28,409
Solanum lycopersicum	08	60	27,000
Total	31	88	30,301

Haplotypic and nucleotide diversities (Table IV) are determined within each individual and for all individuals as a whole. The cytochrome oxidase I (COI) gene reveals high haplotypic diversity and low nucleotide diversity within each population and for all individuals.

Table IV: Haplotypic and nucleotide diversity of each population

Population	Haplotypic diversity (hd)	Nucleotide diversity, Pi(π)
Brassica oleracea	1,000 ± 0,00150	0,07097 ± 0,0000261
Capsicum annuum	1,000 ± 0,00116	0,05981 ± 0,0000102
Solanum lycopersicum	1,000 ± 0,00391	0,05684 ± 0,0000291
Total population	1,000 ± 0,00007	0,06379 ± 0,0000086

2.1.2. Genetic differentiation and structuring

The analysis of genetic differentiation (Table V) shows a value of the degree of genetic differentiation (Fst) negative (-0.02515) and comparable to zero is noted between the population of *C. annuum* and that of *S.*

lycopersicum. On the other hand, low Fst values are recorded between the populations of *B. oleracea* and that of *C. annuum*; between *B. oleracea* and *S. lycopersicum*. The Fst also shows non-significant p-value values between the different host plants.

Table V: Genetic differentiation between populations

Populations	*B. oleracea*	*C. annuum*	*S. lycopersicum*
B. oleracea P value	* *		
C. annuum P-value	0,03429 0,05970	* *	
S. lycopersicum P value	0,02997 0,12989	-0,02515 0,91565	* *

Intra-population genetic distance (Table VI) is higher in individuals of *B. oleracea* (0.063). On the other hand, it is substantially identical in individuals of *C. annuum* and *S. lycopersicum* (0.03). The genetic distance between the populations of *B. oleracea* and *C. annuum* and between *B. oleracea* and *S. lycopersicum* are identical and equal to 0.051. This genetic distance decreases between populations of *C. annuum* and *S. lycopersicum* (0.033).

Table VI: Genetic Distances of Populations

	Genetic distances			
	Intra	Inter		
Populations		*B. oleracea*	*C. annuum*	*S. lycopersicum*
B. oleracea	0,063			
C. annuum	0,037	0,051		
S. lycopersicum	0,034	0,051	0,033	

Analysis of molecular variance (Table VII) reveals a low value of the variance component, a percentage change (1.69723%) not significant and small (p=0.07624) between host plants. On the other hand, the components of the variance are greater within the host plants and the percentage of variation is significantly high (98.30277%).

Table VII: Analysis of Molecular Variance (AMOVA)

Source of variation	sums of squares	Variance components	Percentage change
Between host plants	35,221	0,25855	1,69723 P value = 0,07624
Inside host plants	419,295	14,97484	98,30277
Total population	454,516	15,23338	

2.1.3. Genetic evolution

The analysis of deogenetic indices (Table VIII) reveals positive D of Tajima values and negative Fs of Fu values. The values of D of Tajima and Fs of Fu have P-values well above 5% so the values of D of Tajima and Fs of Fu are not significant. The values of the demographic indices (Table VIII): the sum of the squares of the deviations (SSD) and Raggedness (Rag) are not significant with P-values well above 5%, so there is a gap between the observed values and those expected, then the population is in demographic expansion.

Table VIII: Demogenetic Tests and Demographic Indices

Host plants Demogenetic tests	*B. oleracea*	*C. annuum*	*S. lycopersicum*	Mean	S.d
D of Tajima (P-value)	1,427 (0,95)	1,386 (0,95)	1,231 (0,92)	1,348 (0,94)	0,084 (0,01)
Fs of Fu (P-value)	-1,227 (0,14)	-1,925 (0,12)	-0,465 (0,26)	-1,206 (0,17)	0,596 (0,06)
SSD (P-value)	0,021 (0,27)	0,018 (0,25)	0,022 (0,73)	0,021 (0,42)	0,002 (0,22)
Raggedness (P-value)	0,042 (0,48)	0,036 (0,35)	0,043 (0,87)	0,040 (0,57)	0,003 (0,22)

The two Mismatch distribution curves represent the observed (in red) and expected (in green) frequencies which represents the graphical model of an expanding population) as a function of nucleotide differences between sequence pairs. Analysis of the distribution of genetic distances between individuals of a population taken two to two (Mismatch distribution) shows a multimodal distribution for the three host plants.

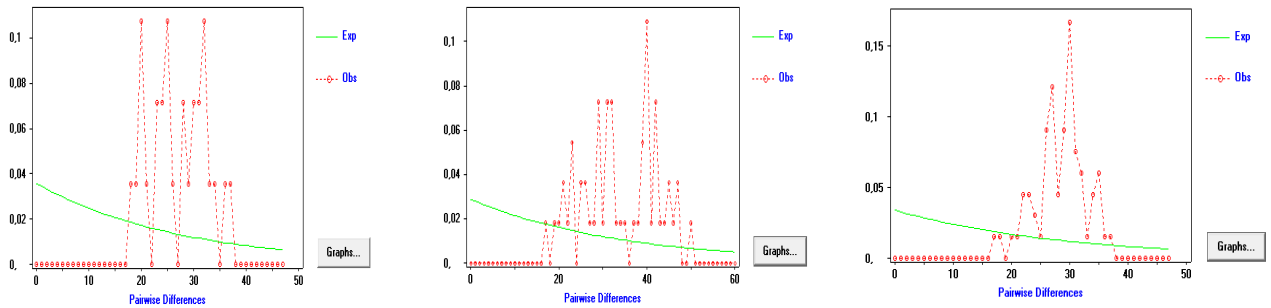

Figure 1: Mismatch curves Distribution

Legend: A: Population of *S. lycopersicum*; B: Population of *C. annuum*; C: *B. oleracea* population

3.1.4. Phylogenetic reconstructions

3.1.4.1. Haplotype network

The dataset is composed of 31 sequences divided into 31 haplotypes that are 99 or even 100% identical to the sequences recorded in the NCBI GenBank database. The haplotype network makes it possible to see the relationships that exist between the haplotypes of the different host plants. Red dots are vectors, i.e. hypothetic haplotypes. The haplotype network shows that all haplotypes are individualized and separated by vectors. The network also shows the presence of three groups of haplotypes and that each group is formed by individuals subservient to the different host plants.

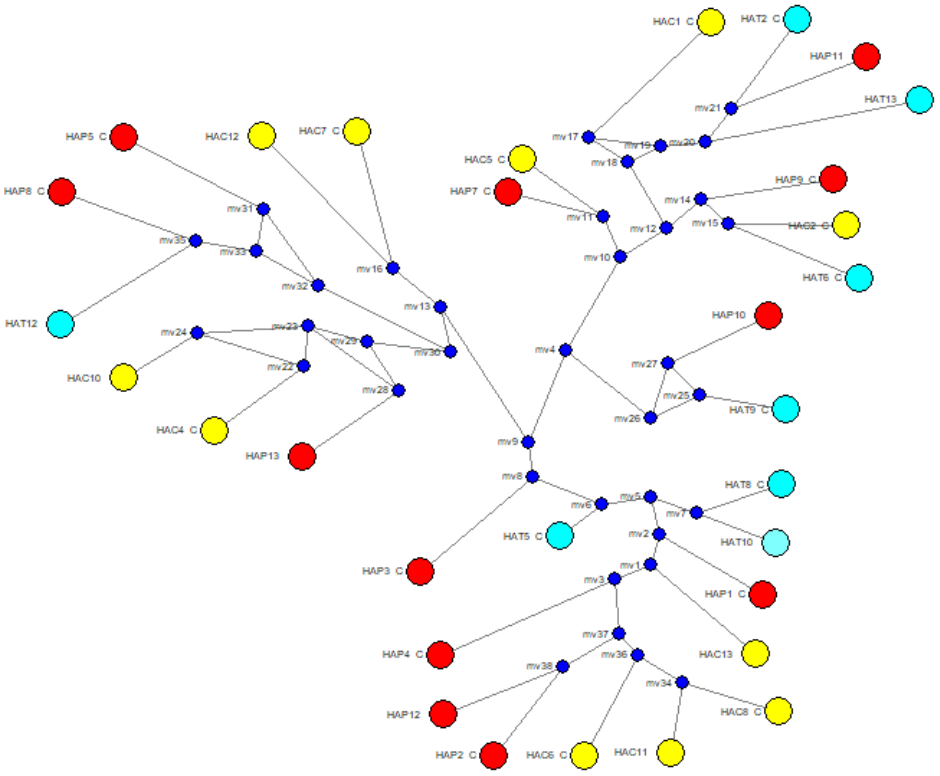

Legend

HaP : *H. armigera* from pepper

HaC : *H. armigera* from cabbage

HaT : *H. armigera* from tomato

Vector

Figure 2: Haplotype network of *H. armigera* populations

3.2.4.2. Phylogenetic Trees

Phylogenetic trees were constructed by the methods of Neighbor-joining, Maximum Parsimony, Maximum Likelihood and Bayesian inference. The phylogenetic tree of Neighbor-joining (Figure 3) shows the existence of two clades C1 and C2 and an unsolved Hac8 individual, i.e. one that is not supported by a boostrap value. The first clade C1 shows the presence of individuals subservient to these three host plants (*B. oleracea*, *S. lycopersicum* and *C. annuum*) which are supported by a high boostrap value (92); while in the second clade C2, only two individuals subservient to the population of *B. oleracea* are observed with a boostrap value equal to 75. By the maximum Parsimony method (Figure 4), the tree follows the same topology as that constructed with the Neighbor-Joining method. The phylogenetic tree of maximum likelihood (Figure 5) also shows the existence of two clades C1 and C2. The C1 clade also shows the presence of individuals subservient to these three host plants that are supported by a high boostrap value (94). The second C2 clade only shows the presence of individuals from *Brassica oleracea* that are supported by a boostrap value equal to 61. This highlights that at the level of *B. oleracea* there is a subpopulation that differs from the others. Bayesian inference (Figure 6) shows the presence of a single clade that follows the same topology as the C1 clades recorded in the other methods and that the hac6, hac8 and Hac11 individuals are not resolved.

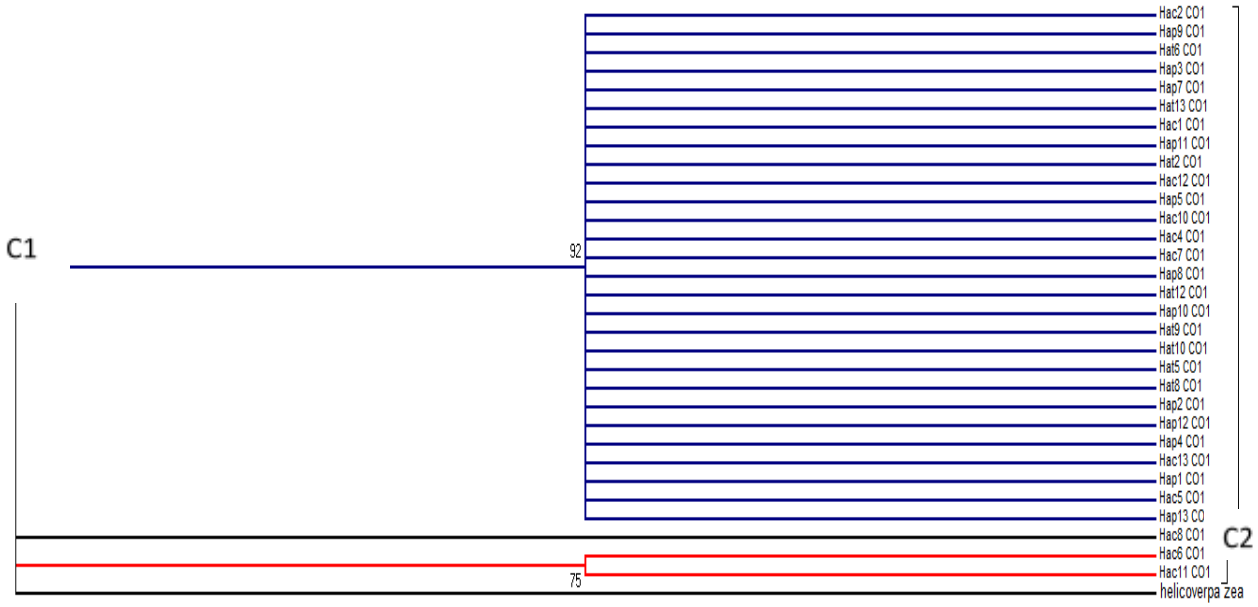

Figure 3: Phylogenetic trees of *H. armigera* individuals by the Neighbor-joining method

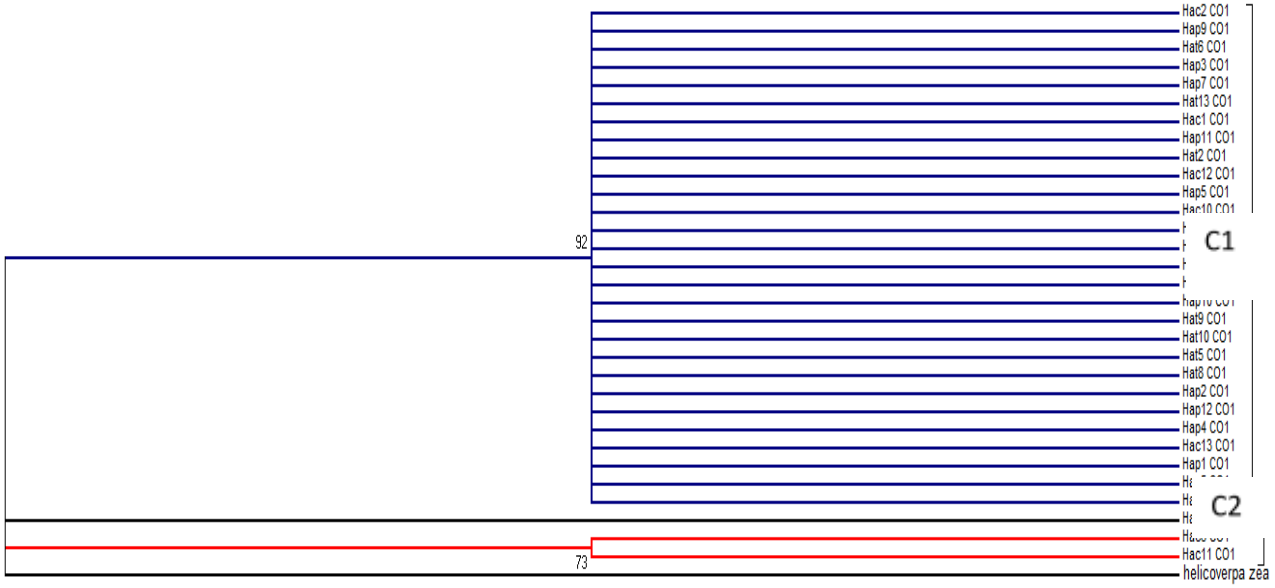

Figure 4: Phylogenetic trees of *H. armigera* individuals by the Maximum Parsimony method

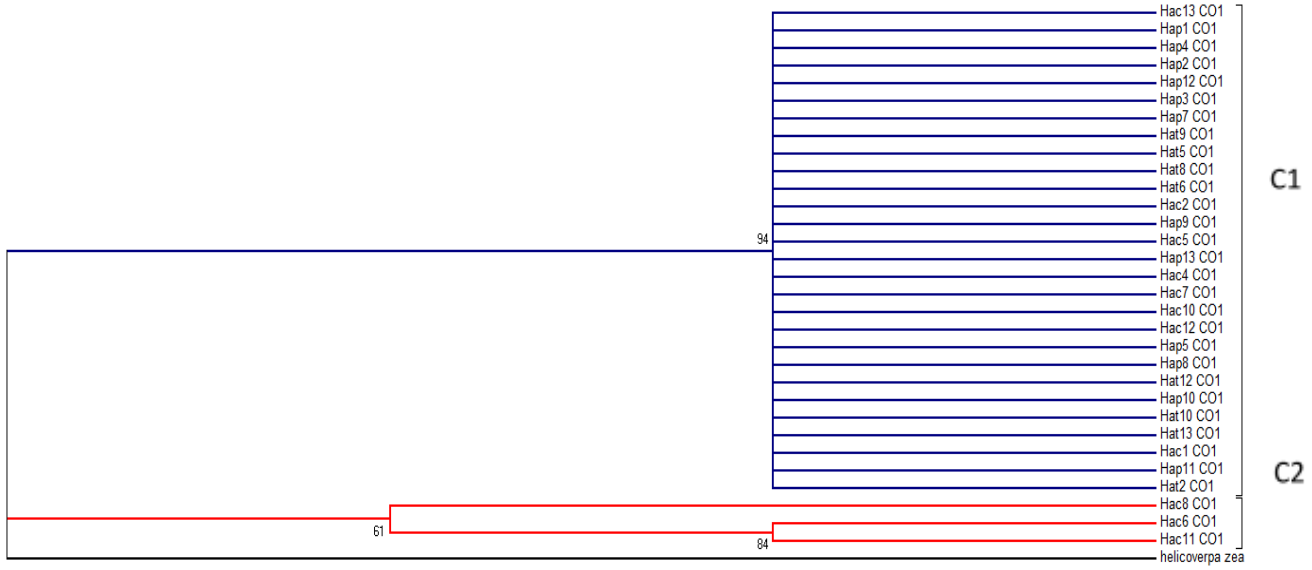

Figure 5: Phylogenetic trees of *H. armigera* individuals using the Maximum Likelihood method

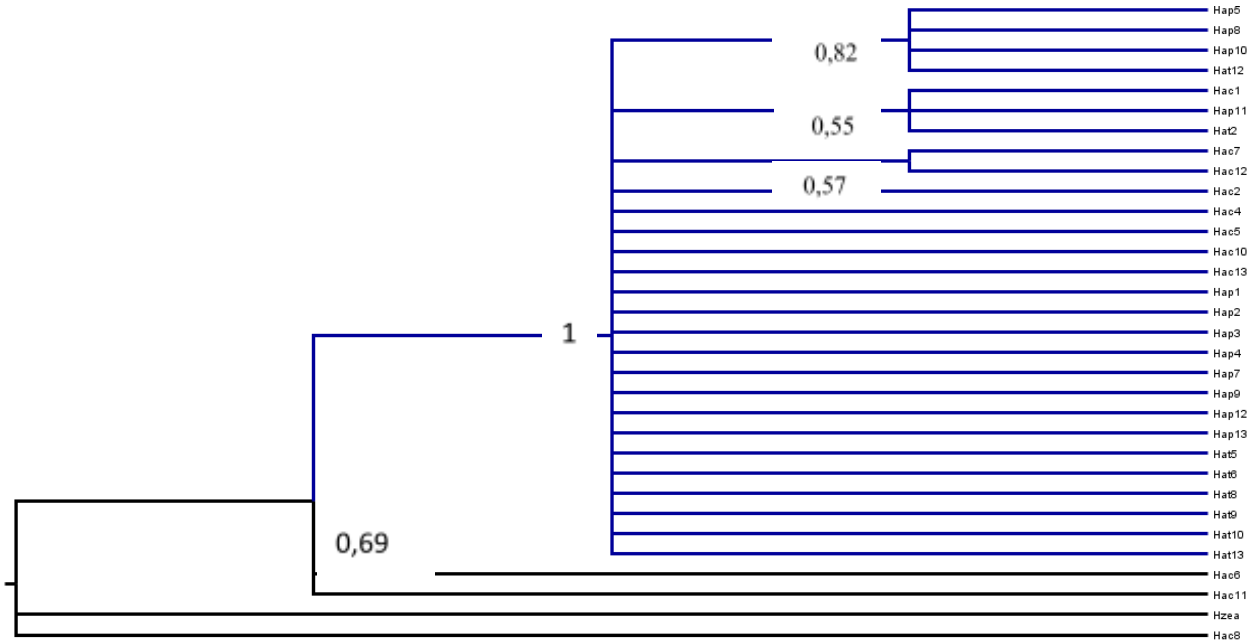

Figure 6: Phylogenetic tree of individuals of *H. armigera* by the Bayesian method

3.2. Discussion

The general objective of this study is to know the genetic diversity and structure of the populations of *Helicoverpa armigera*, a pest of vegetable crops in the Niayes area of Senegal. Analysis of the genetic diversity of *H. armigera* sequences shows that the percentage of transversion (50.96%) is higher than the percentage of transition (49.06%). This leads to a change in amino acids and proteins. The population of *H. armigera* as a whole has high haplotypic diversity and low nucleotide diversity. This could be explained by the signal of rapid population growth from a low-sized ancestral population that has been effective for a sufficient time for a restoration of haplotypic diversity (hd) by mutation, but too short for the accumulation of strong differences between sequences. Populations of *H. armigera* subservient to different plants (*B. oleracea*, *S. lycopersicum* and *C. annuum*) have high haplotypic diversity and low nucleotide diversity. This could be explained by a strong polyphagia, high fecundity [40] and rapid multiplication of the insect that is able to fill up to 10 to 11 generations per year [17]. This high

haplotypic diversity could probably be linked to international trade [49] where imports of agricultural products (maize, sorghum ...) and horticultural (tomato, pepper, cabbage ...) result from the movement of goods. This commercialization allows the population of *H. armigera* from different localities to reproduce and form a population. This was found by [1] which stipulate that commercial movements may not serve as potential entry points for further incursions of agricultural pests. Analysis of the genetic differentiation (Fst) of *H. armigera* populations reveals that there is no genetic differentiation between the different populations of *H. armigera*. This could be explained by the strong migratory capacity of the insect *H. armigera* which can reach thousands of kilometers [16]. Indeed, the insect has a strong ability to spread through a connected landscape and via a hopping dispersion model [2]. These migrations can also allow exchanges between different host plants since the insect *H. armigera* colonizes vegetable and rainfed crops and is able to attack at least 217 species or genera of host plants [35] and caterpillars have a very different impact on different host plants [38]. The Niayes area is characterized by the alternation of two seasons: a wet season and a dry season [12]. Various crops are grown by farmers and *H. armigera* attacks a certain number of horticultural crops in the dry season but tomatoes are the main preferred host plant of *H. armigera*. During the rainy season, the main crops attacked by *H. armigera* are maize, cotton, and sometimes a few individuals attack groundnuts and cowpeas [37]. Given that in the Niayes area, most horticultural crops are practiced from September to June and *H. armigera* colonizes perimeters of vegetable crops such as tomato, cabbage, pepper, lettuce, eggplant ... and peaked in May. Rainfed crops are recolonized by *H. armigera* at the beginning of each rainy season. This asynchronous colonization has been described in West Africa by [37]. Analysis of molecular variance (AMOVA) of the COI gene of *H. armigera* individuals indicates a lack of structuring between host plants. This lack of genetic structuring has been confirmed by [36] which indicates an absence of genetic structuring on a geographical scale. This could lie in a recent extension of the insect's range: there would therefore be admixture between the populations of the different host plants. Indices of demographic change in *H. armigera* populations reveal p-value values well above 5%, which are therefore not significant. This makes it possible to say that the population is in demographic equilibrium or in moderate expansion. Analysis of the distribution of genetic distances between individuals in a population taken two by two (Mismatch distribution) reveals a multimodal curve that indicates a stable population. So the detected expansion would be moderate. The sum of the squares of the deviations (SSD) and the irregularity index (Rag) of the populations of *H. armigera* confirm the hypothesis of a demographic expansion with insignificant p-value values which makes it possible to say that there is a gap between the observed values and those simulated hence the acceptance of the zero hypothesis Ho which indicates that the population is in demographic expansion. Overall, the four methods of phylogenetic reconstructions (Neighbor-joining, Maximum Parsimony, Maximum Likelihood and Bayesian Inference) show congruent results. Indeed, they reveal that individuals are not structured according to the host plant.

IV. CONCLUSION AND PERSPECTIVES

The importance of this study is linked to the fact that it provides the first insights into the genetic diversity of *Helicoverpa armigera* in the Niayes area of Senegal. A great haplotypic diversity was observed between the different host plants. A lack of genetic differentiation was also noted between the populations of the different host plants. Similarly, a lack of genetic structuring between the populations of the different host plants (*B. oleracea, S. lycopersicum* and *C. annuum*) was noted by a small percentage of variation between the host plants. Demogenetic tests indicate the hypothesis of an expanding population and this hypothesis is confirmed by the sum of the squares of the deviations (SSD) and the irregularity index (Rag) of the populations of *H. armigera*. The diversity between individuals from the same host plant deserves to be deepened. Thus, for a better

understanding of the genetic structuring of *H. armigera* in Senegal it is necessary to:

- Expand sample sizes in different host plants to gain insight into the genetic diversity of this insect;
- Characterize the genetic structuring of *H. armigera* using other markers such as microsatellites to determine existing gene flows between host plants in Senegal.

BIBLIOGRAPHIC REFERENCES:

1. Arnemann, J. A., W. J. James., T. K. Walsh, J.V.C. Guedes, G. Smagghe, E. Castiglioni, and W. T. Tay. (2016). Mitochondrial DNA COI characterization of *Helicoverpa armigera* (Lepidoptera: Noctuidae) from Paraguay and Uruguay. Genet. Mol. Res. 2: gmr.15028292.
2. Arnemann, J.A., Roxburgh, S., Walsh, T., Gordon, K., Tay,W.T., Guedes,J., Smagghe, G.(2019). Multiple incursion pathways for *Helicoverpa armigera* in Brazil show its genetic diversity spreading in a connected world. Scientific Reports; 9 ,19380.
3. Arneodo J.D., Balbi E.I., Flores F.M., Sciocco-Cap A. (2015). Molecular identification of *Helicoverpa armigera* (Lepidoptera: Noctuidae: Heliothinae) in Argentina and development of a novel PCR-RFLP method for its rapid differentiation from *H. zea* and *H. gelotopoeon*. J. Econ. Entomol. 108 : 2505-2510.
4. Avise J. C., (2000**)**. Phylogeography : the history and formation of species. Harvard University Press, Cambridge, MA**.**
5. Behere, G. T., Tay, W. T., Russell, D. A., Kranthi, K. R., Batterham, P. (2013). Population genetic structure of the cotton bollworm *Helicoverpa armigera* (Hubner) (Lepidoptera: Noctuidae) in India as inferred from EPIC-PCR DNA markers. PLoS ONE 8: e53448.
6. Collingwood E. F. and Bourdouxhe L. (1980). Trials with decamethrin for the control of *Heliothis armigera* on tomatoes in Senegal. *International Journal of Pest Management* 26, 3-7.
7. Cox, A.J. and Hebert P. D. N. (2001). Colonization, extinction and phylogeographic patterning in a freshwater crustacean. *Molecular Ecology* (10), 371–386.
8. Cunningham, J. P. & Zalucki, M. P. (2014). Understanding Heliothine (Lepidoptera: Heliothinae) pests: what is a host plant. J. Econ. Entomol. 107, 881–896.
9. Czepak, C., Albernaz, C., Vivan, L. M., Guimarães, H. O., Carvalhais, T. (2013). First reported occurrence of *Helicoverpa armigera* (Hübner) (Lepidoptera: Noctuidae) in Brazil. Pesquisa Agropecuária Tropical, 43, 110–113.
10. Decaëns T., Porco D. and Rougerie R., (2013): Le barcoding ADN: un outil pour étudier la biodiversité des invertébrés terrestre. Disponible sur http://www.sfecologie.org/regards/2013/10/15/r50-barcoding-adn-decaens-et-al/. Consulté le 08/12/2020
11. Diallo, M. D., Ngamb, T., Tine, A. K., Guisse, M., Ndiaye, O., Seck, S., Mahamat, S. M., Diallo, A.., Guisse, A., Diop, A. (2015). Caractérisation agropédologique des sols de mboltime dans la zone des Niayes (Sénégal). Agronomie Africaine, 27(1):57–67.
12. Diatte, M., Brévault T., Sall-sy, D., D. K. (2016). Des pratiques culturales influent sur les attaques de deux ravageurs de la tomate dans les Niayes au Sénégal. International Journal of Biological and Chemical Sciences, 10(2): 681–693.
13. Diouf, M., Thioune, P.B.D., Ba, A., E DiawE.B. (2017). Impacts anthropique et climatique sur la dynamique de la nappe des sables quaternaires du littoral nord du Sénégal. Revue du CAMES-Sciences appliquées et de l'ingénieur vol. 2 ISSN 2312-8712.
14. Excoffier L. and Lischer H. E., (2010). A new series of programs to perform population genetics analyses under Linux and Windows. Molecular Ecology Resources 10, 564-567
15. Faye E., 2010, Diagnostic partiel de la flore et de la végétation des Niayes et du Bassin arachidier au Sénégal: application de méthodes floristique, phytosociologique, ethnobotanique et cartographique. Thèse en sciences Agronomiques Université Libre de Bruxelles, Université d`Europe 266 p.
16. Feng, H-Q., Wu, X., Wu B, Wu, K., (2009). Seasonal migration of *Helicoverpa armigera* (Lepidoptera: Noctuidae) over the Bohai Sea.

Journal of Economic Entomology; 102: 95-104.
17. Fitt, G.P. (1989). The ecology of *Heliothis species* in relation to agroecosystems. Ann Rev Entomol 34: 17–52.
18. Fu, Y-X. (1997). Statistical tests of neutrality of mutations against population growth, hitchhiking and background selection. Genetics, 147: 915-925.
19. Gadhiya, H. A., Borad, P.K., bhût, J.B. (2014). Efficacité des insecticides synthétiques contre *Helicoverpa armigera* (Hubner) et *Spodoptera litura* (Fabricius) infester arachide. BioScan; 9 (1): 23-26.
20. Gelman A., Carlin J. B., Stern H. S., Dunson D. B., Vehtari A. and Rubin D. B. (2014). Bayesian Data Analysis. Third Edition. Boca Raton, FL, USA: Chapman and Hall/CRC.
21. Gerszberg, A., K. Hnatuszko-Konka, K., Kowalczyk, T. (2015). In vitro regeneration of eight cultivars of *Brassica oleracea* var. capitata. In Vitro Cell.Dev.Biol. Plant 51: 80–87.
22. Hall, T. BioEdit version 5.0.6. Department of Microbiology, North Carolina State University. (2001).
23. Hebert, P. D. N., Stoeckle, M. Y., Zemlak T. S., Francis C. M. (2004). Identification of birds through DNA barcodes. *Plos Biology* 2: 1657-1663.
24. Herald, K. P., Tayde, A, R. (2018). Biologie et de la morphologie de la pyrale du fruit de tomate, *Helicoverpa armigera* (Hubner) sous Allahabad conditions. Journal of Entomology and Zoology Studies, 6 (4): 1734-1737.
25. Huelsenbeck, J. P. and Ronquist F., (2001). Mrbayes: Bayesian inference of phylogenetic trees. Bioinformatics, (17): 754-755.
26. James, B., Atcha-Ahowé, C., Godonou, I., Baimey, H., Georgen, G., Sikirou, R. and Toko M. (2010). Integrated Pest Management in Vegetable Production: A Guide for ExtensionWorkers in West Africa. International Institute.
27. Kahane, R., Temple, L., Brat, P., De Bon H. (2005**).** Les légumes feuilles des pays tropicaux: Diversité, richesse économique et valeur santé dans un contexte très fragile. Colloque Angers 7-9 septembre 2005-03-14: ''Les légumes: un patrimoine à transmettre et à valoriser Thème III: Utilisation et perception''. CIRAD département Flhor, Bd de la Lironde, 34398 Montpellier cedex 5, 9p.
28. Labou, B. (2016). Distribution des populations de la « Teigne » *Plutella xylostella* (L), du « Borer » *Hellula undalis* (F) et des auxiliaires dans les cultures de chou des Niayes au Sénégal. Thèse, 204p.
29. Librado P. and Rozas J. (2009). DNAsp v5: a software for comprehensive analysis of DNA polymorphism data. Bioinformatics; 25:1451-1452.
30. Lunt, D. H., Zhang, D. X., Szimura, J. M., Hewitt, G. M. (1996). The insect cytochrome oxydase unit I gene: evolutionnary pattern and conserved primers for phylogenetics studies. Insect Molecular Biology. 5 (0), 153-165.
31. Mailafiya, D. M., DegriM. M., Maina Y. T., Gadzama U. N., Galadima I. B. (2014). Preliminary studies on insect pest incidence on tomato in Bama, Borno State, Nigeria. International Letters of Natural Sciences 5; 45–54.
32. Moustier P. (2007). Urban horticulture in Africa and Asia, an efficient corner food supplier. Acta Horticulturae; 762: 145–148.
33. Ndong A., THIAW C., Diome T., Diallo B., Kane M., Sarr M. and Sembène M. (2015). Barcoding: Comparison of Variation Degree of COI and Cytochrome b Mitochondrial Markers in Two Species. Primary Maize Pests (*Sitophilus zeamais* and *Sitophilus oryzae*).
34. Nei, M. (1987). Molecular evolutionary genetics, *Columbia University Press*, New York. NY, USA.
35. Nibouche S., 1999. Montpellier: CIRAD-CA, 56 p. (Déprédateurs du cotonnier en Afrique tropicale et dans le reste du monde, 12) ISBN 2-87614-314-3
36. Nibouche S., 2009. Lutte intégrée contre les insectes ravageurs du cotonnier et de la canne à sucre: caractérisation et gestion des interactions culture - insecte à l'échelle de la plante, du peuplement végétal et de l'agroécosystème: Document de synthèse présenté pour l'obtention de l'Habilitation à

diriger des recherches. Saint-Denis: Université de la Réunion, 47 p.3
37. Nibouche, S., Natacha,G., Pierre,M., & Vaissayre,M. (2006). Modélisation du rôle des refuges pour la gestion durable du coton Bt à double gène dans les systèmes agricoles de l' Afrique occidentale. ScienceDirect; 26(2007): 828–836
38. Pearce, S. L., Clarke, D. F., Est, P. D., Elfekih, S., Gordon, K. H. J., Jermiin, L. S., Mcgaughran, A., Oakeshott, J. G., Papanikolaou, A., Perera, O. P., Rane, R. V, Richards, S., Tay, W. T., Walsh, T. K., & Anderson, A. (2017). Open Access innovations génomiques, la plasticité de la transcription et de la perte de gènes qui sous-tendent l'évolution et la divergence des deux très polyphage et invasive *Helicoverpa* espèces nuisibles. BMC Biology: 1–30.
39. Rambaut UN., 2014 Figtree, un visualiseur graphique d'arbres phylogénétiques [Internet]. Disponible sur : http://tree. bio.ed.ac.uk/software/figtree.
40. Razmjou, J., B., Naseri., Hemati. S.A. (2014). Performances comparatives du ver de la capsule du coton, *Helicoverpa armigera* (Hübner) (Lepidoptera: Noctuidae) sur diverses plantes hôtes. J. Pest Sci; 87 : 29-37.
41. Sharma, H.C. (2001). Cotton bollworm/legume pod borer, *Helicoverpa armigera* (Hubner) (Noctuidae: Lepidoptera): Biology and management. Crop Protection. Compendium. CAB International, Wallin-gford, 70p.
42. Sharma,V. G., Kumar,.S. (2019). Biologie des *Helicoverpa armigera* (Hubner) sur tomate dans le Gujarat Sud. Jounal of Entomology and Zoology Studies; 7(5): 532–537.
43. Shi Q-H., Zhao F., Hao J-S. and Yang Q. (2013). Complete mitochondrial genome of the Common Evening Brown, *Melanitis leda* Linnaeus (*Lepidoptera: Nymphalidae: Satyrinae*). Mitochondrial DNA, Informa UK, Ltd.
44. Silaste, M. L., Alfthan, G., Aro, A., Kesäniemi, Y. A., & Hörkkö, S. (2007). Tomato juice decreases LDL cholesterol levels and increases LDL resistance to oxidation. British Journal of Nutrition; 98(6): 1251–1258.
45. Smith, O.B., CIRAD (Organization). (2004). Développement durable de l'agriculture urbaine en Afrique francophone enjeux, concepts et méthode. Centre de coopération internationale en recherche agronomique pour le développement; Centre recherches pour le développement international, Paris; Ottawa.
46. Spicer G. S. (1995). Phylogenetic utility of the mitochondrial cytochrome oxidase gene: molecular evolution of the *Drosophila buzzatti* species complex. J. Mol. Evol; 41: 479-759.
47. Tajima, F. Statistical method for testing the neutral mutation hypothesis by DNA polymorphism. Genetics. (1989). 123: 585-595.
48. Tamura, K., Peterson, D., Peterson, N., Stecher, G., Nei, M. & Kumar, S. "MEGA 5: Molecular Evolutionary Genetics Analysis using Maximum Likelihood, Evolutionary Distance, and Maximum Parsimony Methods". Molecular Biology and Evolution. (2011). 28 (10) : 2731-2739.
49. Tay, W. T., Walsh, T. K., Downes, S., Anderson, C., Jermiin, L. S., Wong, T. K., Gordon, K. H. (2017). Mitochondrial DNA and trade data support multiple origins of *Helicoverpa armigera* (Lepidoptera, Noctuidae) in Brazil. Science Reports*; 7,* 45302.
50. Thompson, J., Higgins, D., Gibson, T. (1997). CLUSTAL W: improving the sensitivity of progressive multiple sequence alignment through sequence weighting, position-specific gap penalties and weight matrix choice. Nucleic Acids Research; 22: 4673-4690.
51. Wang, C. Y., Feng, Y., Chen X. (2012**).** Complete sequence and gene organization of the mitochondrial genome of *Batocera lineolata* Chevrolat (*Coleoptera*: *Cerambycidae*); 57(27) : 3578- 3585.
52. Wares, J.P. and Cunningham, C.W. (2001a). Comparative phylogeography and historical ecology of the North Atlantic intertidal. Evolution; 55: 2455-2469.
53. Wares, J.P. and Cunningham, C.W. (2001b**).** Phylogeography and historical ecology of the

North Atlantic intertidal. Evolution; 12: 2455–2469.
54. Yi, D., Cui, L., Wang, L., Liu, Y., Zhuang, M., Zhang, Y., Zhang, J., Lang, Z., Zhang, Z., Fang, Z., Yang, L. (2013). Pyramiding of Bt cry1Ia8 andcry1Ba3 genes into cabbage (*Brassica oleracea* L. var. *capitata*) confers effective control against diamondback moth. Plant Cell Tiss Organ Cult 115: 419–428.
55. Yolou, I., Yabi, I., Kombieni, F., Tovihoudji, P.G., Yabi, J.A., Paraïso, A.A., Afouda, F. (2015). Maraîchage en milieu urbain à Parakou au Nord-Bénin et sa rentabilité économique. Int. J. Innov. Sci. Res; 19(2): 290-302.

Possibilities to Overcome Negative Attitudes Towards Immunization Against Covid-19

Dr. Galinka Ivanova Pavlova, MD

University of Sofia

ABSTRACT

Surveys of public sentiments show that Bulgarians are the most skeptical about immunizations against Coronavirus, which is why our country is among the last places in the EU in terms of vaccination coverage. The aim of this study is to identify the causes of negative attitudes and to formulate recommendations for effective solutions that raise the reliable public awareness and minimize skepticism. Both documentary and sociological methods were used in the study. 459 people were interviewed and 43 in-depth interviews were conducted within the period of November-December 2021. Conclusions and recommendations: The absence, for a long time, of a national system-structured information campaign and the later misconducted one, combined with a wave of infodemia, are the main reasons for the negative sentiments about the vaccination against Covid-19. The creation of permanent information centers in settlements and the opportunity for personal contact of citizens with locally proven medical authorities will help to overcome the negative attitudes.

Keywords: infodemia, Covid-19, attitudes, immunization.

Classification: DDC Code: 330.973 LCC Code: HC106.5

Language: English

London Journals Press

LJP Copyright ID: 925693
Print ISSN: 2631-8490
Online ISSN: 2631-8504

London Journal of Research in Science: Natural and Formal

Volume 22 | Issue 6 | Compilation 1.0

Possibilities to Overcome Negative Attitudes Towards Immunization Against Covid-19

Dr. Galinka Ivanova Pavlova, MD

SUMMARY

Surveys of public sentiments show that Bulgarians are the most skeptical about immunizations against Coronavirus, which is why our country is among the last places in the EU in terms of vaccination coverage. The aim of this study is to identify the causes of negative attitudes and to formulate recommendations for effective solutions that raise the reliable public awareness and minimize skepticism. Both documentary and sociological methods were used in the study. 459 people were interviewed and 43 in-depth interviews were conducted within the period of November-December 2021. Conclusions and recommendations: The absence, for a long time, of a national system-structured information campaign and the later misconducted one, combined with a wave of infodemia, are the main reasons for the negative sentiments about the vaccination against Covid-19. The creation of permanent information centers in settlements and the opportunity for personal contact of citizens with locally proven medical authorities will help to overcome the negative attitudes.

Keywords: infodemia, Covid-19, attitudes, immunization.

Author: Assoc. Prof. Faculty of Public Health Medical University of Sofia.

I. INTRODUCTION

For more than two years now, the world has been living in a Covid-19 pandemic. The application of vaccines against the virus that causes the disease is a crucial part of the possibility to handle this challenge. In this regard, the Government of the Republic of Bulgaria has ensured the availability of sufficient quantities of AstraZeneca, Pfizer and Moderna vaccines approved for use in Europe. Surveys of public sentiments show that Bulgarians are the most skeptical about immunizations against coronavirus, which is why our country is among the last places in the EU in terms of vaccination coverage. According to data of the Unified Information Portal, as of 30.04.2022, 4,386,264 doses have been administered. The total number of persons having gone through a completed vaccination course is 2,055,820 (29.6% of the population in the country). We are also last in the administration of booster doses. Considering the average percentage for the EU countries being 51.4%, the revaccinated persons in Bulgaria are only 10.8% of the population [1]. Unfortunately, the phenomenon of "fake vaccinations" poses a problem for many EU countries [8]. Bulgaria does not make an exception, from where it follows that the officially reported number of immunized persons is probably lower, given the existence of bad practices for reporting immunizations without such having been performed at all.

Insufficient vaccination coverage is also a worrying issue for the migration process. Over the last decade, "since the European Parliament adopted a Resolution on promoting worker mobility within the EU (2010/2273 (INI)), migration processes have increased, especially among young people." In order to avoid reckless risks, it is imperative that the conditions of residence in the country we want to go to [4] are studied carefully. This implies the obligation and responsibility to comply with anti-epidemic measures, including through mass vaccination, introduced at both national and European levels, in order to control the Covid pandemic.

The many unknowns in the outbreak of the pandemic relating to the diagnosis, treatment, complications and vaccination against Covid-19, as well as the anti-vaccination sentiments, have sparked a worldwide wave of misinformation and fake news reaching the public through various communication channels [2]. The World Health Organization (WHO) defined the rapid spread of this type of malicious information as "infodemia", which can be even more dangerous than the virus itself [7,8].

National vaccination campaigns in most European countries started as early as December 2020 and gave good results in terms of high vaccination coverage. Only at the end of March 2022, the Ministry of Health launched an information campaign "+ me" about the benefits of vaccines and vaccination against Covid-19. Within the initiative, a website www.плюсмен.бг has been created, where everyone can find answers to the questions they ask themselves in connection with the pandemic and vaccines [5].

Despite the efforts of experts and institutions, at European and national levels, to change negative attitudes, the problem of non-vaccination remains persistent. This determines the relevance of the topic related to the study of the possibilities for helping to overcome the skepticism among the Bulgarian population regarding the immunization against Covid-19.

The aim of the study is to identify the causes of negative attitudes and formulate recommendations for effective solutions that raise the reliable public awareness of vaccination against Covid-19 and minimize skepticism.

In order to achieve the aim thus set, the following tasks need to be solved:

1. To study and analyze the motives for refusing vaccination;
2. To identify the preferred sources of communication;
3. To study the impact of personal consultations with a medical professional on attitudes towards immunization.

II. RESEARCH METHODS

Both documentary and sociological methods were used in the research study. Data from an anonymous standardized questionnaire survey conducted among 459 people who attended informative talks held in enterprises from the city of Varna, as well as 43 in-depth interviews with men and women aged 40-65 conducted after public consultations, were analyzed by the author of the article personally, in the period November-December 2021.

The study does not claim to be representative, however, it provides an opportunity to identify the main reasons for the hesitation and skepticism about vaccination against Covid-19, to identify trends related to trust in the health system and the pharmaceutical industry, and to formulate recommendations for reducing the number of people with negative attitudes.

III. EMPIRICAL VERIFICATIONS

Insufficient activity in the vaccination process in the country has been reported due to the following reasons:

- No national information campaign;
- Initially misrepresented information creating increased expectations in people to prevent infection with the virus after application of vaccines and discrepancy between those attitudes and reality;
- Contradictory media messages from various experts;
- Growing lack of trust in the government, institutions and experts discussing the topic.

As a result, the Municipal Council of Varna decided to hold informative talks and consultations among citizens in order to raise awareness with scientifically proven facts about the benefits of vaccination, possible side effects and contraindications for various diseases [6]. During this period, representatives of the municipal medical establishments involved in the campaign held more than 60 meetings which were attended by over 1,500 people and consulted over 170 people. In three of the company teams with talks held (Public Transport EAD, Municipal

Waste Processing Plant EOOD and secondary school), some of those present (459) responded to the invitation to participate in a survey and in a direct interview (43).

In the distribution of the respondents by gender and age, men predominated (83.5%), which can be explained by the nature of the respondents' work. The largest share (49.9%) were persons aged 55-65 years, followed by those aged 40-55 years (39.6%), those up to 40 years of age were 7.3% and those over 65 years - 3.2%. Respondents with secondary education predominated (74.6%), 21.2% were those with higher education and 4.2% with primary education. More than a third of the respondents (38.9%) reported having some chronic illness.

Those who had gone through Covid-19 represented 39.6% of the respondents, 13.1% were not sure if they had it, and 47.3% categorically denied to have had it. A significant proportion of patients (71.8%) were diagnosed through antigen and/or PCR tests, 22% reported having antibodies after being tested, and 6.2% had not tested but had the typical symptoms of the disease.

The share of vaccinated persons among the respondents (with one or two doses administered) was only 12.6%, with a significant part (77.1%) not planning to be immunized (49.4% NO + 27.7% Rather NO) (Fig. 1)

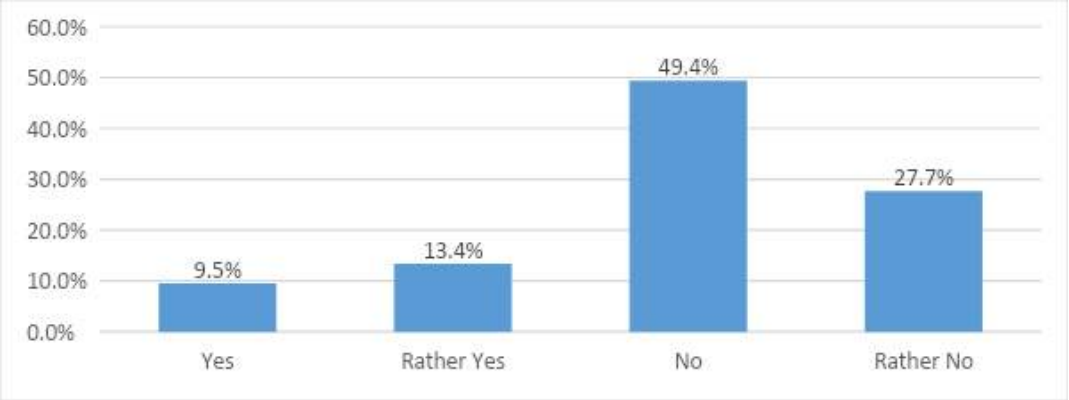

Fig. 1: Do you have any plans to get vaccinated against Covid-19?

Respondents with a categorical decision to be immunized were five times less than those who had a categorically negative answer.

Quite a few of the respondents (68.5% = 41.7% YES + 26.8% Rather YES) reported having concerns about their health as a result of immunization. Only 17.6% were at peace about their health after vaccination and gave a categorically negative answer, while 13.9% expressed some doubts. Respondents' fears were related to allegations spread through various communication channels, most often the Facebook network. The largest share (74.5%) were those who were concerned about the "short period of creation of the vaccines", 47.6% about the "formation of blood clots" and 25.2% about subsequent "infertility". Respondents' concerns were also related to "DNA change" (14.2%) and "individual chipping" (7.5%). The anxiety and tension in a large part of the respondents (39.9%) was caused by the requirement for signing an "Informed Consent" by the immunized, which, according to them, released the pharmaceutical company from liability in case of any complications after vaccination.

The most common and accessible sources representing the main information channel are the television media (63.6%), a significant role is played by communication with relatives and acquaintances (34.9%), followed by social networks (32.8%), physicians (including GPs) (28%) and others (11.4%). Respondents expressed varying degrees of trust in information sources (Fig. 2).

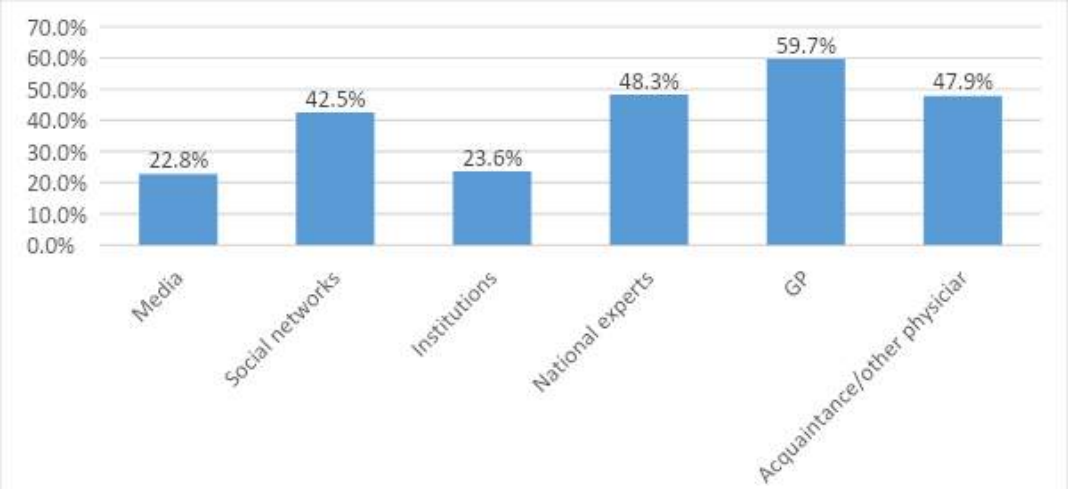

Fig. 2: Which of the following information sources do you trust? (more than one answer is possible)

GPs (59.7%), national experts (48.3%) and acquaintances/other physicians (47.9%) were the most trusted. Although the media and social networks are the main sources of information, trust in them is not high. It is noteworthy that the respondents had more trust in social networks than in the media. The least trust was registered in institutions (23.6%).

From the graph in Fig. 3 we learn about the benefits of the respondents' participation in educational meetings.

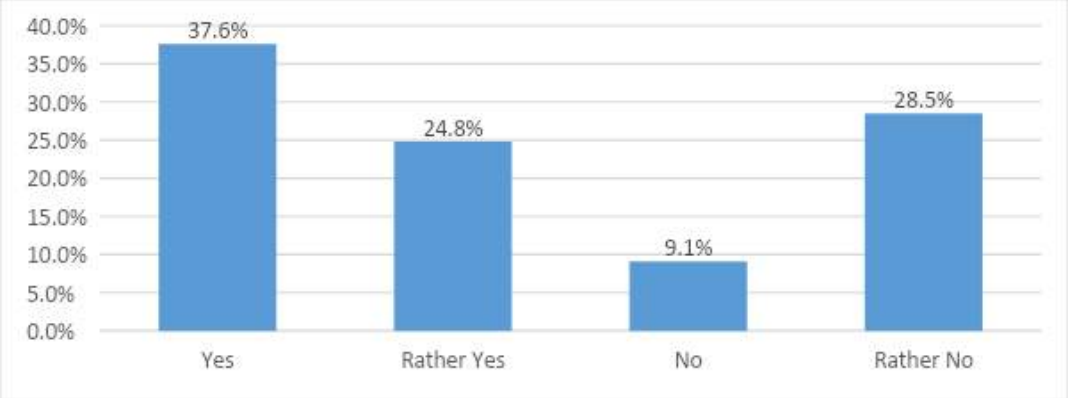

Fig. 3: During the informative talk, did you receive answers to the questions about the vaccination against Covid-19 which cause you concern?

More than half of the respondents (62.4% = 37.6% + 24.8%) were satisfied with the information presented during the organized talks and received a satisfactory answer to the questions that concern them. Only 9.1% were categorically disappointed.

A significant part of the respondents (73.4%) reported that they would like to receive personal advice on issues related to vaccination and their personal health (Fig. 4).

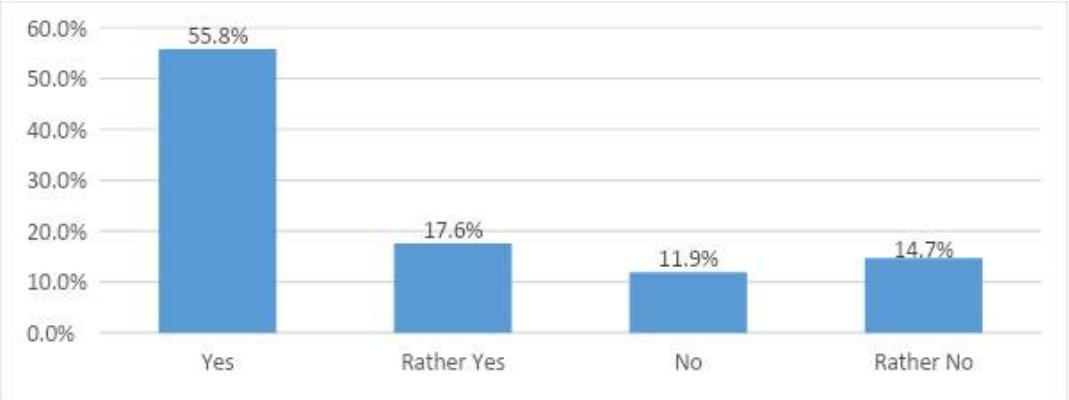

Fig. 4: Would you take the opportunity to have a personal consultation with a physician/GP about the vaccination of you and/or a relative?

A quarter of them (26.6%) were not interested in further information that they could receive in individual consultations.

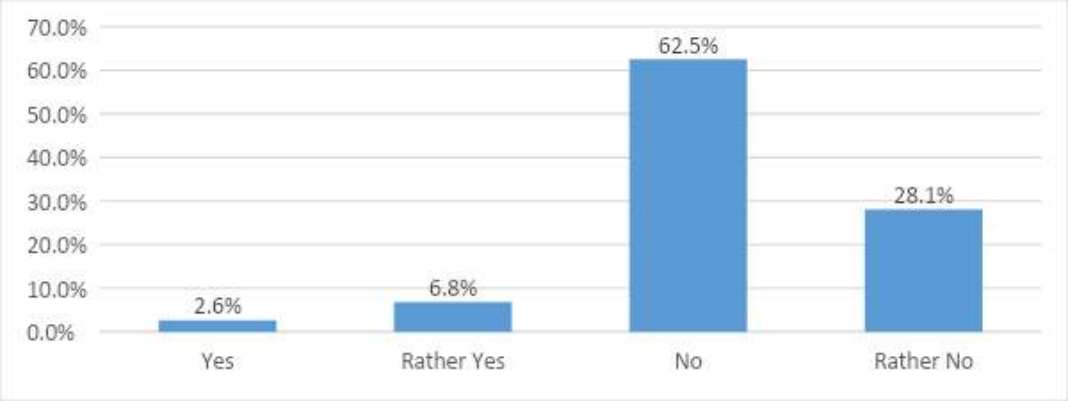

Fig. 5: If you answered NO to the first question, did the informative talk change your attitude towards vaccination?

Despite the approval of the informative talk by a large part of the respondents, only 2.6% reported a change in their attitude towards the vaccination against Covid-19, while those being hesitant but having a positive attitude was another 6.8%. The share of those who denied the need for immunization, keeping their negative attitude unchanged, remained significant (90.6% = 62.5% NO + 28.1% Rather NO).

The results of the direct interviews conducted confirm the trend of the anonymous survey. Dominant reasons for refusing vaccination were: "not tested enough", "quickly appeared on the pharmaceutical market", "I am not sure how they will affect my health". The majority of the participants stated that Covid disease was a "global conspiracy" caused by the "financial interests of the major pharmaceutical industries". Skepticism was heightened by the lack of trust in the "government" and the "health care system". Most interviewees wished to use "personal consultation", "have contact with a physician they know and trust", "discuss the specific risks to their health", "ask about their chronic illness and that of a member of their family", "choose which vaccine to get" and "when the right time is to get immunized". The possibility of "feedback from a known physician", "consultation in case of side effects" would "reduce the tension and fear of the unknowns" related to immunization and would "give a sense of security and peace of mind".

Within a month after the informative meetings and personal consultations conducted, 19 respondents sought assistance from the author and were vaccinated in the immunization office of the municipal medical establishment which organized part of the educational talks. The lack of uniform information about all those present at the informative meetings and about any possible subsequent vaccinations of some of them do not allow to assess the effectiveness of the municipal program.

IV. CONCLUSIONS

The absence, at the beginning of the pandemic, of a national, system-structured information campaign and the later misconducted one, combined with the lack of trust in government and institutions, as well as a wave of infodemia spreading mainly on social networks, are among the main reasons for the existence of negative attitudes towards the vaccination against Covid-19.

V. RECOMMENDATIONS

Overcoming skepticism is only possible by:

- Joining the efforts of all stakeholders at both national and local levels in conducting the information campaign.
- Establishing permanent information centers at various locations where medical specialists will consult citizens on vaccination, while checking their health.
- Involving locally proven authorities and maximum level of spread of reliable information among users.
- Strengthening personal contact and feedback between citizens and the physician they trust.

Conclusion: Since the spring of this year, we have seen a significant decline in the incidence of Covid-19 in all countries, which has led to the abolition of a number of restrictive and anti-epidemic measures. Unfortunately, scientists' concerns about the development of the next pandemic wave in the fall remain. Conducting a national campaign in a new way, bringing the information about the Covid-19 vaccines as close to the people as possible, will help change attitudes among those who are hesitant.

BIBLIOGRAPHY

1. Unified information portal - https://coronavirus.bg
2. Karabova-Hambarova I., N. Mateva, Covid-19 - Information and Infodemia on Social Media: Online Research. Health Policy and Management, 2020, vol. 20
3. Kineva T., Vaccines against Covid-19 through the eyes of Bulgarian citizens. Economic and Social Alternatives, 2021.
4. Kolev N., Mobility of Young People - Trends, Factors, Effects and Risks, Collection of reports from an R&D project of the Research Fund, University of Ruse "Angel Kanchev", 2016
5. Ministry of Health - https://www.Nh.govermment.bg
6. Varna Municipal Council - https://varnacouncil.bg
7. Petrova S., Infodemia, Fake News and Post-Truth. Southwestern University "Neofit Rilski"
8. Sidzhimova D., Infodemia in a COVID-19 Pandemic. Health Policy and Management, Vol. 1, 2021, pp. 22-27

Simplifying Physics Mathematics Research Methodology

Rajan Iyer

ABSTRACT

This expository physics research methodologies will not involve extensive literature surveys of currently employed practitioners' research methodologies. Rather a way or technique to simply a new approach to minimize paper trail, keeping algorithm gist while overriding cumbersome mathematical elaborations will be main theme of this article. However, this may provide a beneficial outlet to programmable algorithmic methods having a step by steps derivative applied quantitative physics modeling that has the power to pull out proof verifiable as well as measurable observables. Pure mathematicians then can apply these conjectures to a more rigorous, highly involved extensive proof processes protocol.

Keywords: NA

Classification: DDC Code: 332 LCC Code: HG173

Language: English

London Journals Press

LJP Copyright ID: 925694
Print ISSN: 2631-8490
Online ISSN: 2631-8504

London Journal of Research in Science: Natural and Formal

Volume 22 | Issue 6 | Compilation 1.0

Simplifying Physics Mathematics Research Methodology

Rajan Iyer*

ABSTRACT

This expository physics research methodologies will not involve extensive literature surveys of currently employed practitioners' research methodologies. Rather a way or technique to simply a new approach to minimize paper trail, keeping algorithm gist while overriding cumbersome mathematical elaborations will be main theme of this article. However, this may provide a beneficial outlet to programmable algorithmic methods having a step by steps derivative applied quantitative physics modeling that has the power to pull out proof verifiable as well as measurable observables. Pure mathematicians then can apply these conjectures to a more rigorous, highly involved extensive proof processes protocol.

The author realizes that it is beyond the scope of the current article to engage in extensive literature review surveys. However, relevant literature references have been listed to help the scientific readership to clarify key points. The author is ready to write sequel articles to clarify queries that will help to foster creativity important expositions, explanations, scientific norms, and shifting paradoxes. Philosophically as well as scientifically transforming present situations, the author will also then focus on factors of global importance. An Invitation requesting publications and, or presentations, the author will address these issues extensively.

**Author:* Environmental Materials Theoretical Physicist, Department of Physical Mathematics Sciences Engineering Project Technologies, Engineeringinc International Operational Teknet Earth Global, Tempe, Arizona, United States of America. ORCID ID#:0000-0002-5729-1393.

I. INTRODUCTION

Historically, the author has been an experimental materials researcher in graduate and postdoctoral projects. The methodology adopted there had always been aimed at economical; however, essentially efficient innovative ways and techniques that will reduce operational costs while generating results that have scientifically significant outcomes. The trick was then applied fundamental properties to model experiments with a maximum simplicity approach. Designing experiments with observable identified critical parameters form the basis of successful observations, measurements, analysis, and usefully commercially relevant scientific results.

Theoretical Physics that the author has carried out involves fundamentally ansatz novel approaches to solve quantum, relativity, and classical physics, which have presented currently various resulting inconsistencies. Researching thoroughly physics literature, the author has been able to think deeply aloud the logic constituting the backbone of the physics. Coming up with Helmholtz decomposition of fields onto mechanical gradient and the vortex fields have been the pointer to the prime key to an ansatz formalism, which had physical observables tangibly towards gaging to equivalent electromagnetic fields. The author has solved the problem of identifying the fundamental physical mechanism that generates energy universally in a perpetual, albeit dissipative, discontinuous manner. This work has been conducted by working with scientists worldwide. Various articles relating to this research have been recently published, after scientific peer-review process. These publications highlight a model of Pauli-Dirac-Planck circuit assembly operator. This operator presents a proposed

mechanism of generating energy at subatomic to Planck quantum level, and functions as a clocking mechanism. It is an energy generator via action of the monopole-particle magneto-electric fields. Modifications of the original theoretical model provided a conjugation of Scalar Theory of Everything authored by scientist John Hodge in the form of hod-Plenum-PDP assemblies. Global physical-mathematical scientists O'Neill, Malaver, Zhang, Hodge, and Taylor were collaboratively co authoring with the author to come up with quantification of an Integrated Model. Such an Integrated Model incorporates mesoscopic observables to verify validity of the model. This extensive paper has been recently peer-reviewed and published by the prestigiously well-esteemed Canadian Journal of Pure and Applied Sciences.

Science, specifical physics, has logic bases to rationalize qualitative versus quantitative argumentations with programmable situational computing values. To compare logic, we require at least a common property or parameter. An example will explore oft-stated quote "…. We can't compare apples and oranges….". To compare them, we will have to use their standard classification of groups, which in this case, they belong to the fruit classification. Another example is "Which one came first – egg or chicken?". In this example, we will have to have a common ingredient to compare, which is the carbon basis of life itself!! When we have examples with people, female and male, comparisons become murky. Only traits may have common comparisons like their offsprings or reproduction, which generally are female and male generations. Essentially, genetics and species classification of organisms come under the science of taxonomy, and that will have to be explored as such.

When the logic of classical, relativistic, and quantum physics are compared, they have inherent inconsistencies, amplified to the well-known general problem of vacuum or ultraviolet catastrophe. The author has logically identified quantum energy density metrics to be the common property or parameter. Presently the vacuum solutions point to key parameter of signal/noise density matrix to bring quantum physics within the same platform with general relativistic physics. The author has expatiated about it in the subsequent section of the current article.

II. ARGUMENTATION, RESULTS, and DISCUSSIONS

2.1 Logic of Mind Over Matter Nature

Logicality, correct and valid reasoning in the study of logic,advances within the current article by exemplifications of a matrix – constant or a dynamic representation of the motion of objects. The conundrum is the extremum of a riddle or a mystery; paradox is an extremum of a puzzle. They form the dual sides of a matrix!!An example of a mystery is the above quoted classification of groups "Which one came first – egg or chicken?", versus the example of a paradox "Schrodinger's famous cat!!". One solution to the riddle solution is mentioned above is coming up with an identifying common ingredient, carbon; one of the solutions of a paradox such as "Schrodinger's cat" is in recognizing leakage quantum wave functions, occurring via the walls of the box; it will help to identify the life state of the cat!! We will have to overcome the measurement problem to achieve that with Schrodinger Equation in conjunction with the Heisenberg Uncertainty Principle!! *In deep philosophical sense, mathematics evanesces,by itself, set of belief systems borne out of logically explainable things, often known in terms of fuzzy logicality versus not-fault logicality!!*

(Consciousness)of)mind)over)matter)time)space)sense)

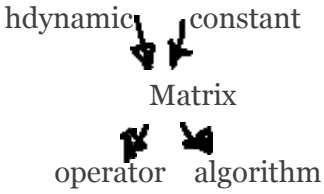

It may appear that consciousness ~ sense, time ~ sounds, light ~a vacuum (~ denotes association with), and space has associations with all!! In terms of PHYSICS, time+space has four dimensions, while sense may well represent the five dimensions altogether!! Hence, consciousness manifests wholesomeness of existence!!

2.2 Will technology help to simplify everyday life?

We know technology has active input coming via science as well as art. While many technological products such as apps, devices, structures, establishments, computers, and guidance systems have made our everyday tasks easier, perhaps they still have user-end complexities. The year 2022 may herald having simplifications applied technologically.

[What?]{Take trivial space out of the information timeline}

[Why?]{Clog and mess up working space otherwise}

[How?]{Justify typical relevance of that space specifically, significantly to keep or clean up}

Scientifically applying extreme value statistics projection operator matrix with "Proof Formalism…" Algorithm, that author derived must be a part of pure mathematics helping to simplify the wide range of tasks within applications. These are mentioned in the article listed below in Referential Literature as a first principle simplifying technique.

Metaphysical aspects with physical mathematics here may have philosophical implications with Hindu Mythology having "$3\tilde{\infty}$" {representing Omm….}, the primordial sound of the universe as central operator with "Brahma Saraswathi" flowering outwards, then "Lakshmi-Vishnu" and the Trinity Siva-Parthi, creating real universe!!

One-way logical understanding of consciousness might generate via thought, symmetrically conjugatively asanti-thought. Psychological aspects with physiology implied by the phrase "mind over matter", for example,typically reveals denouement reality. Physiological aspects with psychology, like minds reading themselves while engaging with other minds, perhaps tells us how entangled they can be!! One may envisage quantum decoherence or entanglement to guide physiological, psychological interactive processes!!

(PDP)circuit)mind)of)universe)protocol)operator)metrix?)

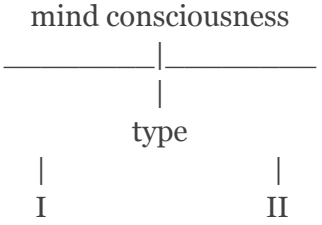

.["What?" "Why?" "How?"] {Many conditions must be satisfied to have life existing}. While a type I may be a guesser, a type II may be a thinker!!.... containment of mind over matter is vital!!

2.3 Image of human outer consciousness!!

Type I with image switching having speed of light may have much sooner than type II with sound switching vibrations at the rate of sound. That is why a guesser beats out a thinker, probably!!

Hence, type I decision-makers will have about 10,000 times as fast as type II decision-makers to call out, like the stock market!! For example, a type I decision-maker or a guesser may take only one minute while type II decision-maker or a thinker may take almost a week to give out an answer!!Especially if a type I is a lucky guesser!!

ALGORITHMIC GAGE THEORETICAL PHYSICAL MODELING [Referential Citations Literature Shortlist 1-20] Rethinking Physics: General Quantum Gravity

Equating broken telephone network information: $$\sum_{i=1}^{n}\sum_{j=1}^{m}\Gamma_{ij}=1 \quad (1.1)$$

with Γ_{ij}: signal/noise ratio of i, j element of information transmission line matrix.Equation (1.1) is a constitutive equation quantifying how multiple matrices relates to one another. For example, in the case of entanglement versus decoherence based on critical Γ property, the Equation (1.1) conforms onto a unitarized principle of conservation of energy in the quantum relativity realm.

Point dynamics PHYSICS dissipative theory Iyer Markoulakis & Equation of gage discontinuity per Iyer O'Neill Malaver Hodge Zhang Taylor physical modeling

$$\mathbf{G}_g=\boldsymbol{\rho}_{PDP}(t_g)\,(\langle\boldsymbol{\Psi}_{\mu}(t_g)|\boldsymbol{\Psi}^{\mu}(t_g)\rangle)^{-1}\quad_{GR} \quad (1.2)$$

In Equation (1.2), $\mathbf{G}_g$ represents the gage functional linking, $\boldsymbol{\rho}_{PDP}$ represents the Pauli-Dirac-Planck (PDP) quantum density matrix, $(\langle\boldsymbol{\Psi}_{\mu}(t_g)|\boldsymbol{\Psi}^{\mu}(t_g)\rangle)$ represents the inner product matrix of wave functions under variable μ and t_g represents the gage time domain; $_{GR}$ represents the gage space field. Point to point information energy transmissions are possible with vortex gradient process; however, energy -> entropy with the conversion of potential energy to kinetic energy with such transmissions are possible with emergent temperature rises' transformations!! Rationalizing broken telephone network, Equation (1.1) and the functional Equation (1.2) is exemplified by an observable example of mesoscopic level of analogy to quantum aspects have been given in the Appendix III of the author's paper in Canadian Journal of Pure and Applied Sciences, coauthored by five other scientists. This demonstrable observable exemplifies with the case of ducks and the swans' population pattern swimming together in a lake; "bra-ket" product matrix values within the Equation (1.2) are given in Equation (2),characterizing row-column form, like it is in the esteemed Canadian Journal of Pure and Applied Sciences(CJPAS) article in Appendix II.

$$\langle\boldsymbol{\Psi}_{\mu}(t_g)|=\langle\boldsymbol{\Psi}_{d}(t_g)|=\langle\boldsymbol{\Psi}_{ducks}(t_g)|;|\boldsymbol{\Psi}^{\mu}(t_g)\rangle=|\boldsymbol{\Psi}^{s}(t_g)\rangle=|\boldsymbol{\Psi}^{swans}(t_g)\rangle \quad (2)$$

because ducks are in a "row" and swans go in a direction "column" swimming together!! Note:ρ_{ds}represents population density pattern constituting ducks and swans, **Gg represents** functional having sound, light, and modon{known to transmit in water per article in the CJPAS journal} strings, $_{GR}$ represents gage fields typically{gradient, vortex} up and down pressure and temperature. Typically, gradient takes the real value in the form of the temperature and the pressure is the real value of the vortex fields. We can picture this with the following communication connection logic to language quipping: swans sense the ducks making scenes!!

Picturing algorithm expansion matrix equating

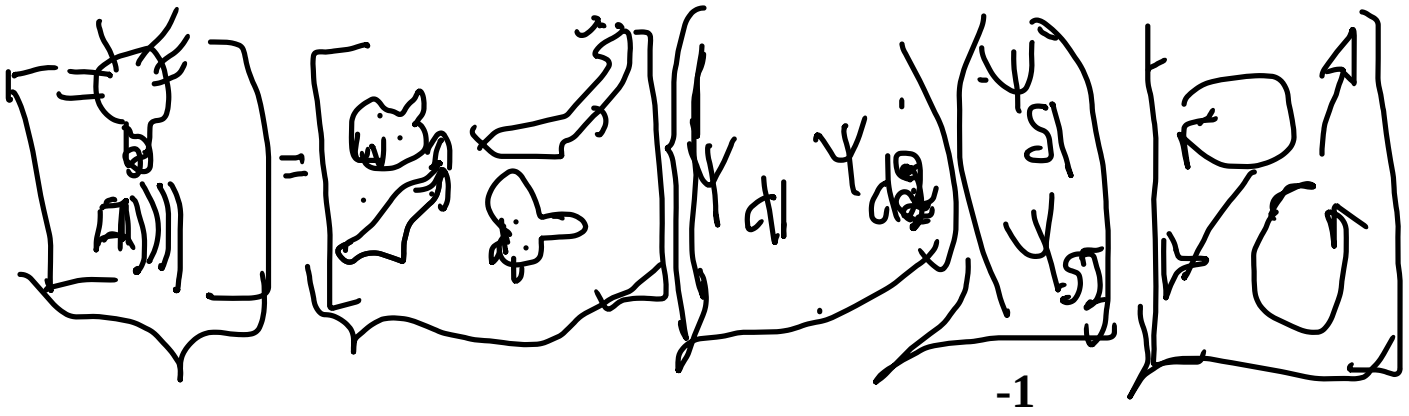

$$\mathbf{G}_g = \boldsymbol{\rho}_{ds}(t_g)\,(<\boldsymbol{\Psi}_d(t_g)|\boldsymbol{\Psi}^s(t_g)>)^{-1}{}_{GR}$$

Having that the "ducks on a row": $<\Psi ducks(tg)|$ = ($\Psi d1$ $\Psi d2$), then column "swans on arrow": $|\Psi swans(tg)>$ = 

Gradient fields are the up/down temperature. Vortex fields have anticlockwise-clockwise pressure.

Quantum gage gravity and multiverse physics modeling theory Critical quantum signal/noise density matrix may explain Smartnews reference on double-slit experiment as particle/wave, whether sensor on/off, i. e. watching observer versus experimenter!!

Typical "ket" matrix for complex angular momentum with {off, on} switching modes, giving signal/noise "Γ" at any point "Γ_{point}" with [point] = {states and/or modes} Example here: Ψ^i: component wave-function imaginary, Ψ^ω: component wave-function angular momentum, Ψ_{off}&Ψ_{on} are component wave-functions of switches modes off&on, and $\Gamma_{i,off,on,\omega} \equiv \Gamma_{point}$, having [point] = {i, off, on, ω}variable gives following algorithm equation operationally [21]:

$$|\Psi i\ \Psi\omega>(\Psi_{off}\ \Psi_{on}) =>: :<= ([\{(\Gamma i,\ off,\ on, \omega)\}]) \quad (3)$$

Equation (3) will apply to momentum space sense. Algorithmically, with time space, we write:

$$|\Psi i\ \Psi^{\omega}>(\Psi_{real}\ \Psi_{proper}) =>: :<= ([\{(\Gamma i,\ \omega,\ proper,\ real)\}]) \quad (4)$$

Where {i, ω, proper, real} = $[point]_{warping}$ or $\Pi_{warping}$ since point-to-point multiplication proceeds magic square prime number factorization processes.Hence

$\Pi_{warping} = [\Pi_{XYZ}]$, equivalent metrically operator=>: : <= $[\Gamma_{X'Y'Z'}]\,[\Gamma_{X''Y''Z''}]$ ..... (5)

With $[\Gamma_{XYZ}]$ =>: : <= $[\Gamma_{X'Y'Z'}]\,[\Gamma_{X''Y''Z''}]$ ....., with $\{\Gamma_{X'Y'Z'}, \Gamma_{X''Y''Z''}\} > [\Gamma_{XYZ}]$, where Γ ≡ signal/noise on XYZ coordinates with primes denoting differentiated coordinates [21]. We write, point in place general equation having "Γ_{point}" with [point]≡ {latitude, longitude} observable.

Equation (4) shows how momentum transfers between sense-space to time-space by switching signals that will carry information energy point to point. From Iyer Markoulakis's formalism, an issue is either

London Journal of Research in Science: Natural and Formal

a zero-point or a microblackhole [2]. Time will typically slow down at a black-hole entity with extreme gravity [https://profoundphysics.com/why-time-slows-down-near-a-blackhole].Mathematically interpreting the physics within the Equations (4) & (5) we can hypothesize that point-to-point inflation with multiplicative processes {magic square prime number factorization} induce a zero-point space having a proper time and a micro blackhole space having the real slow down time. Information energy flow happens, communicating switches' modular signals between zero-point to microblackhole. Thereby it would establish looping!!From the author's earlier publication articles [20, 21], we know that gravity oscillations occur because of signal/noise density matrix either multiplying/inflating or combining/compacting actively in comparison with the critical matrix. With Equations (4) & (5) demonstrating looping due to information flowing point-point between zero-point and microblackhole, one can together conceive of a loop gravity model, per physics literature, providing grand unifying theories within physics literature[https:// en.wikipedia.org/ wiki Loop_quantum_gravity].

Analysis of Equations (3) & (4) will give us more insights of the physics.We realize that while the Equation (3) characterizes momentum space sense, the Equation (4) characterizes time-space.Performing intersection operation, i.e., Equation (3) ∩ Equation (4), we get resultant: $|\Psi i \quad \Psi^{\omega}\rangle$ =(momentum space-sense) ∩(time-space)≡ space ≡ $([\{(\Gamma i,\ off,\ on, \omega)\}])\cap([\{(\Gamma i,\ \omega,\ proper,\ real)\}])$(6) However, these are different categories. Mathematically, then a functor might characterize "space" aspects. Regarding the literature about functor algebra, one may write using [https://www.math3ma.com/blog/what-is-a-functor-part-1]: "functor F:C→D from category C to a category D consists of some data that satisfies certain properties. The Data: (i) an object F(x) in D for every object x in C;(ii)a morphism $F(x) \xrightarrow{F(f)} F(y)$in D for every morphism $x \xrightarrow{f} y$ in C. The Properties are that:(i)F respects composition,i.e., $F(g\circ f)=F(g)\circ F(f)$ in Dwhenever g and f are composable morphisms in C; (ii) F sends identities to identities, i.e., $F(id_x)=id_{F(x)}$for all objects x in C", like schematically has appeared there [https://www.math3ma.com/blog/what-is-a-functor-part-1]. We apply this functor algebra to the Equation (6) to obtain the equivalent operations:

$$F(\Psi^{i})F(f)\longrightarrow F(\Psi^{\omega})F(\Psi^{i})\longrightarrow F(f)F(\Psi^{\omega}) \qquad (7)$$

Therefore, we map functor algebra with Equation (7):

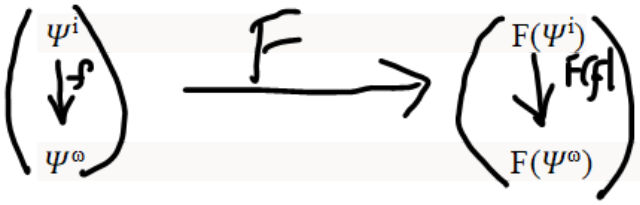

Map (1)

Defining $F(\Psi^{i}) = ([\{(\Gamma i)\}])$ & $F(\Psi^{\omega}) = ([\{(\Gamma\omega)\}])$, one may rewrite Map (1):

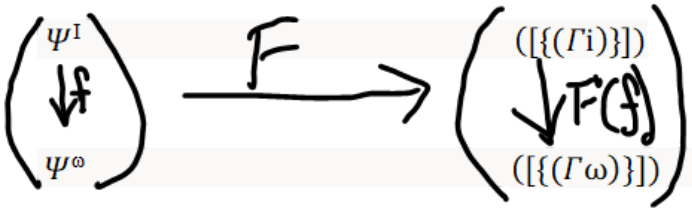

Map (2)

Map (2) will tell us that the point-to-point signal/noise "Γ" density matrix of each category will connect via functor F (f) operator having composable morphisms with an Infinitum multiverse vectorially adding as sense⊗time⊗space dimensions. Therefore, Ψ^{i} representing imaginary component of the wavefunctions link via f toΨ^{ω} representing component angular momentum of the wave functions to translate with the functor action F on ([{(Γi)}]) to ([{(Γω)}]). If zero-point ([{(Γi)}]) characterizes the gradient of field signal/noise density matrix, then ([{(Γω)}])represents rotation of field signal/noise density matrix. Hence, these essentially correlate to Helmholtz's decomposition of the field to the gradient and the rotational fields that Iyer Markoulakis's formalisms [2] quantify zero-point inflationary gradient fields versus microblackhole rotational vortex fields, as Helmholtz's decomposition of point fields.The point gradient vortex model [2] has dissipative properties [6]. Map (2) characterizes discontinuous properties, that the functor operator algebra of the point physics model emphasizes ultimately as gage physics.

Metaphysically, Equations (3) & (4) can be transformed by having i = consciousness of the mind = proper, ω = experience of the real = body. We transform the Equation (4) to:

$$|\Psi\text{consciousness } \Psi\text{experience}> \ (\Psi_{body}, \Psi_{mind}) =>: :<= \\ ([\{(\Gamma consciousness,\ experience,\ mind,\ body)\}]) \tag{8}$$

(hconscious, experience) ≡ [awareness]

Much like physics, metaphysics Equation (8) will tell us that each point can be either consciousness or experience of mind or body, although there are four possibilities. Like physics, metaphysical interpretation will say to us that there are two logical possibilities only, i. e., either human experience or mind consciousness with the body representing human existence in real nature in a geodesic environment!! The four aspects get fulfilled once we realize that there is type I & type II mind consciousness, schematically argued above. Extending to human experience, we may perceive kind of type I' or type II' body experience: possibly still or body meditative type II' states or body active or instinctive type I' states!! These are part of physical reality [22, 23].Summarizing these aspects with a simple schematic of how inorganics get coupled to organics are shown below. In this schematic, fibrational strings are borne out of superluminous plenum hod-PDP circuit assemblies [6] that can generate living structures. One may surmise that really the human experience naturally perceives space action timeline event sequences. Note that in this schematic, (material) represents "living" units likely with {sodium, potassium, phosphate, bicarbonate} compounds, and "modon"{known to transmit in water per article in the CJPAS journal} represents fibrational strings connecting "tubules".

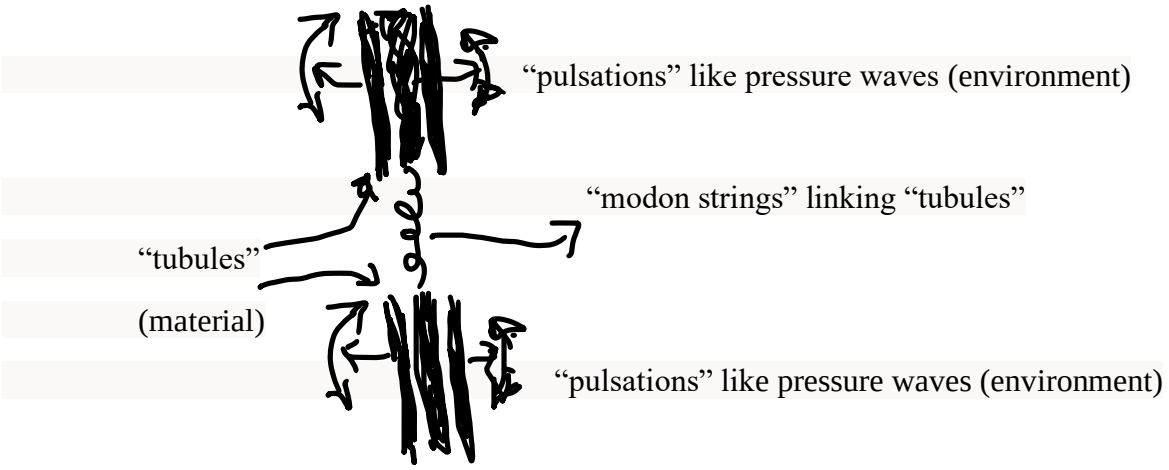

In this schematic scenario, one can hypothesize the following. Signal/noise "Γ" at any point is computable from the Equations (3) through (7). They signify origination of linking the point formalism to astrophysics [1-24] to get a simplified M [X] = [Y] M-theory like graphic matrix theory mapping astrophysical observed phenomena from gage metrics of the potential quantum wavefunctions, described above. We can write compactly these results as logicality algorithm.

$$\Psi_{mapping} = F(\Gamma_{point}) \text{ and } \varphi_{mapping} = G(\Psi_{mapping}) \ldots\ldots\ldots \quad \text{(AFAM.I)}$$

Acronym "AFAM" will mean"Algebra Functor Algorithm Mapping" that will help in computer programming!! (AFAM.I) is an equation that yields the following coordinate algebra formula.

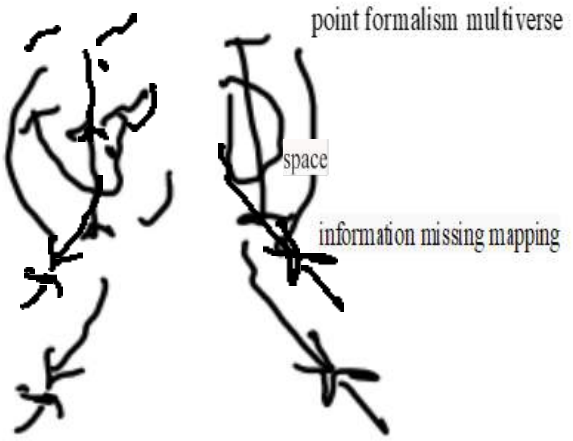

This Coordinate algebra formula can possibly quantify H. G. Well's "Time Machine"to represent a "worldline" hinting really "tomorrow" like wavefunction-potential coordinate of space-time-sense. They merge quantum to astrophysics to enable gage metrics mapping.

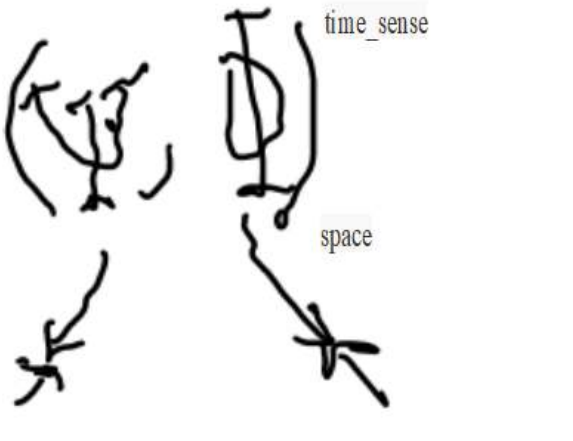

This type algorithmic mapping will help towards Physical Sciences Algorithm IT Programming.

gradient, vortex =>: :<= 

With g_{μ} gage photons like $\Psi_{gradient}$, while $\mu_{\nu\nu}$ phonons are like Ψ_{vortex}, forming point density matrix equivalent to point signal/noise Γ gradient vortex [21] and Equations (3) & (4). Gage photons arise from gradient uncertainty point physics, while phonons arise out of vortex uncertainty point physics. Note that gage function g is with the functor μ, which is linked by the functional ν representing the modon{known to transmit in water per article in the CJPAS journal} strings. Like SUSY $\mu_{\nu\nu}$ equivalently is symmetric with ν.However, asymmetry is generated by hod-PDP Plenum mechanistic aspects [6]. Hence $\mu_{\nu\nu}$ =>: :<= $\mu_{\nu\nu'}$. Aspects thus ensure antiparticle particle asymmetry to create an observable universe!!The ν modon strings phonon-photon versus the ν'modon{known to transmit in water per article in the CJPAS journal}strings photon-phonon have asymmetric relationships!! These conjectures will have eventual proofs, theoretical mathematically and experimental practically with verifications, exemplifying earth interstellar observable cosmic microwave background radiations!!
$\Pi_{differential\ matrix:}$ If [Γ] < [Γcr], then it will differentiate or split-separate onto multiple phases matrices, where [Γ] is a critical signal/noise density matrix, gage unitarized, especially for point [20]. In vacuum, this process will create zero-point matrices since the vacuum will keep absorbing signals making [Γ] < [Γcr], thereby keep generating a$\Pi_{differential\ matrix}$.On the contrary within a nebula, this process will create microblackholes by having higher noise levels thereby making [Γ] < [Γcr], causing zero-point matrices gradient fields generations repeatedly.

Analysis, like above, will yield resultant g_{μ} gage photons like $\Psi_{gradient}$, while $\mu_{\nu\nu}$ phonons are like Ψ_{vortex}, forming point density matrix equivalent to point signal/noise Γgradient vortex. Γpoint gradient vortex will generate electron-positron and, or monopole particle pairs to create PDP circuit assemblages, stabilizer at the quantum level to perpetual generators of energy, and then conversion of energy to matter particles [2, 6, 20, 21]. Accretions of the point particles to quantum particles will be enabled and enhanced by having [Γ] > [Γcr]. Thus, multiple phases matrices mix, combine or synthesize into more complex forms. One primordial aspect example will be not only the creation of electron-positron pairs out of the above schema at the central standard observable zone but also originating quarks and the gravitons from these primordial particles with photon mediating. Fermions and the bosons hence can be hypothesized to form from their primordial dark counterparts. These counterparts are conceivable as particle and antiparticle dark-fermions and dark-bosons.They form manifesting theory of algebra functor linking by a functional the gage function units, per operator algebra matrix protocol quantifying Physical Sciences, discussed above.

We have thus so far discussed possible process mechanisms by which primordial particles,and their particle spectra may be created primarily from a universal vacuum and a nebula. The criteria of signal/noise density matrix explained above defines $\Pi_{differential\text{-}matrix}$versus $\Pi_{accretion\text{-}matrix}$, with gradient and the vortex action fields of point matrix [2-6, 10, 11, 20, 21] deciding operational process genesis parameters!! Step-by-step algorithmic formalisms have been originally derived from the pure mathematics of logical protocol matrices and the pure physics of observations. Foregoing discussions have brought out possibility of how real universes may originate from the asymmetry of particle and antiparticle. We have also discussed briefly about modon{known to transmit in water per article in the CJPAS journal}strings and they can asymmetrically interlink gage photons with phonons. One point of caution also will become evident from perfectly non assumptive derivations able to generate observables that were demonstrated by a possible physical observation in mesoscopic level {per

Appendix III of the CJPAS paper}. This will hint at parity while comparing throughput and output with input. We would expect that they would shift asymmetrically, i. e. indicating a possible mismatch or incommensurability underlining what physicists are facing as measurement problem. This may be manifesting also as paradoxes of well-known double-slit experimental measurements of light interference patterns. Altogether, they may appear as CPT problem, i.e., charge, parity, time reversal situations making it difficult for physical scientists to interpret theory with experimental measurements. However, these ideally derived algorithms will cross-check the results of observation measurements versus observables to correct for inconsistencies. As brought out clearly in the derivation of observables [6], the g_{μ}metrics of the gage photons are like $\Psi_{gradient}$, and the μ_{vv}metrics of the phonons are like Ψ_{vortex}.These parameters are obtainable from signal/noise density matrix. It is quite pertinent to note from a practical standpoint, usually the only measurable parameter in astrophysical observable signal matrix. Therefore, Γrepresenting the signal/noise gradient vortex density matrices probably will be ideal variable to be analyzed by fundamental micro-macro matrix physical algorithm [4, 7]. We should also, however, note that computation of inverse matrices is involved for evaluating gage action fields [6]. We may be lucky in considering 2x2 product matrices, for which inverses can be easily evaluated. Hence the 2x2 algorithmic matrices {emphasized per Appendix III of the CJPAS paper} are amenable to perfect analyses of operational process parameters, such as temperature and pressure variables that are in conjunction with photon-phonon gage physics. These mesoscopic observable gaging fields characterize Equation of motion of observable objects responding to environmental stimuli. Partial differential equations obtained from point physics [2] are transcendental in even most straightforward cases of problem-solving with attractive and repulsive force fields [25] to translate equation of motion objects equivalently. These processes are paramount to the grand unification efforts within the physics characterizing natural quantum astrophysics. The approach that the author has undertaken working with the international scientific community's eminent coauthors will help towards achieving that goal. Presently discontinuous physics has been advanced progressively to relate various functor aspects with spatial existence of matter, physical reality, and mind consciousness awareness!! These may point to multiverse possibility of theorizing coexistence of dark energy, dark matter, and compounding with real observable universal matter [12. 19, 24]. Appendix Database at the end of this paper article briefly outlines scenarios per the above scheme of PDP, particle, antiparticle, dark-particle, and dark-antiparticle game theory. Typically, tic tac chess game perpetual-motion-machine types of situations have been schematically depicted there. In the background hod-Plenum progenitor Infinitum superluminous aether-type medium implies to provide underlying support base like grounds [6]. Mathematically only gage differential, and typically no higher-order differentials are possible due to discontinuous physics [22].

$$\begin{pmatrix} \hat{\varepsilon}_{r,\mu\nu} & \hat{\varepsilon}_{g}^{\mu\nu} \\ \hat{\varepsilon}_{g,\mu\nu} & \hat{\varepsilon}_{r}^{\mu\nu} \end{pmatrix}$$

gaged to the gradient field, quantum density, and the wave functions of point matrix [2], may be rewritten as a point vortex gradient field Dirac matrix, that is signal/noise gradient vortex matrix, equivalently, given in the form of a sketch here.

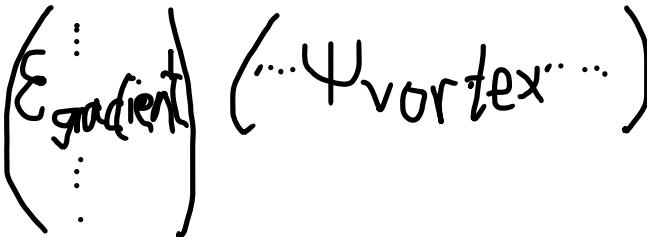

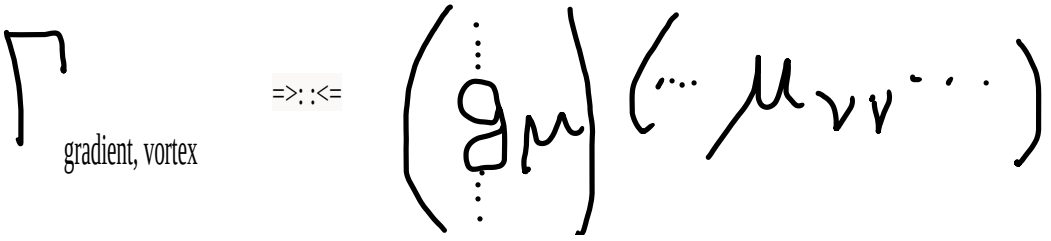

Time in the matrix extended form can be obtained from the" Γ" factor and the gravity Π_{gg} metrics to give a 2x2 matrix of the form

$$\begin{pmatrix} \hat{t}_{pr,\mu\nu} & \hat{t}_{g}^{\mu\nu} \\ \hat{t}_{l,\mu\nu} & \hat{t}_{r}^{\mu\nu} \end{pmatrix}$$

Note that $\hat{t}_{pr,\mu\nu}$ represents proper time, $\hat{t}_{r}^{\mu\nu}$ represents real-time, $\hat{t}_{g}^{\mu\nu}$ represents global time, and $\hat{t}_{l,\mu\nu}$ represents time at local level. You may refer to event timeline explanation in the "*Referential Citations Literature Shortlist*" section below.

Algorithmic derivation potential gaging wavefunction-potential coordinate algebra: (Ψ, φ)

Gaging (Ψ, φ) with algebra [6] gives g[(Ψ, φ)] ≡ (Ψ,), having g[Ψ] ≡ Ψ, since wavefunctions already in the form of unitary gage!! and that g[scalar potential] is a gaging field because field byproper physics original logical definition is a differential space potential.

(Ψ,) essentially means: = f(Ψ), which is valid for dissipative hod-PDP circuit [6] that has a clocking function; however, one hod-PDP assembly is a functor to another hod-PDP assembly linked by algebra functional like G [3-7] in the Equation (1). Functor aspects are vital to quantifying discontinuous physics!!

Four vector matrix form physics

$$\begin{pmatrix} \cdot \\ \varepsilon_{gr} \\ \cdot \end{pmatrix} (.\psi_{\omega}.) =>::<= (.\ \Gamma_{\omega,gr}\ .)$$

or rewriting this will mean that (. $\Gamma_{\omega,gr}$.) associates with

$$(.\,\Gamma_{\omega,gr}\,.) =>: :<= \begin{pmatrix} . \\ \varepsilon_{gr} \\ . \end{pmatrix} (.\,\psi_{\omega}.).$$

Practically,only signal/noise astrophysics are measurable observations, that is pointed out above.This relationship of "$\Gamma_{\omega,gr}$" matrix to split matrix form of "ket-bra" product matrices of "ε_{gr}" and "ψ_{ω}" are ideal to be transformed to gage spatial fields gradient and the rotational wavefunctions matrices. Typically, gradient gage spatial electromagnetic fields are convertible toward having switching fields with mode {0, off, on}, so that

$$\begin{pmatrix} . \\ \varepsilon_{gr} \\ . \end{pmatrix}$$

matrix will appear as [ ]{0, off, on} form or as numerical matrix:

$$\begin{pmatrix} 0 \\ \emptyset \\ 1 \\ \phi \end{pmatrix}$$

In this "ket" four-column matrix"0" would refer to zero fields,"∅" would refer to neither {off} or {on} fields,"1" would refer to {on} fields, and"ϕ" would refer to both {off} and {on} fields. These are perhaps physics, reminiscent of modern quantum physics, characterizing entangled quantum fields.

Rotational vortex matrix $(.\,\psi_{\omega}.)$is a matrix representation of rotational sense wavefunctions, designated as[Ψ] matrix. Then, sense is classified to be {clockwise, anticlockwise, positive, negative}. Symbolically, they can be written in the form of a matrix such as

$$(\psi_{\circlearrowright},\ \psi_{\circlearrowleft},\ \psi_{+}\psi_{-}).$$

Based on these notations, we may write signal/noise matrix to fields-wavefunction gage unitarized matrices equation to be in the form of signal/noise matrix with rotational "ω" and the gradient "gr" subscripted notations. Therefore,

$$(.\,\Gamma_{\omega,gr}\,.) =>: :<= \begin{pmatrix} 0 \\ \emptyset \\ 1 \\ \phi \end{pmatrix} (\psi_{\circlearrowright},\ \psi_{\circlearrowleft},\ \psi_{+}\psi_{-}) \qquad (I)$$

We note that we can figure out the 4x4 four vector-matrix form of quaternion algebra with ϕ≡ i.

Algorithm (I) is a four vector-matrix form of 4x4 quaternion matrix physical mathematics. This has the power to quantify Γrepresenting critical signal/noise density matrix andρ representing flavor density matrix of mass M in the string-metrics, described elsewhere [20] in the sections"Critical (Γ, ρ) matrix electromagnetic gravity keying parametrically" from "Gage time gage space fields probability signal matrix". Algorithm (I) when used per formulations [20] in conjunction with field-matter metrics will help to facilitate transformations among observables, observations, and measurements that are achieved by experimental or natural methods. These are widely applicable then to astrophysics and

quantum physics parameters of potential and the wave functions that may be operating at mesoscopic or other normal physics levels!!

Gage's cursory look of the Algorithm (I) and the Equation (1) will tell us that while electromagnetic force appears as signal profile field matrix, gravitational force appears as density matrix time-space manifesting flavor with mass factor and both together in string-metrics [3, 4, 10]. Practically achieving with typically observations measurements having spectral density alongside intensities signal profiling will be then part of experimental physics.

The above-explained 4x4 quaternion matrix physical mathematics characterizing gaging fields and the wave functions would be incorporating detailed elements of micro-macro mathematics. Among them space, charge, and complex fields of astrophysical to quantum electromagnetic and gravity fields will be involved that may be in a state of entanglement or decoherence. They may involve either or both wave function possibly in quaternion forms. Because of their physics being algorithmically quantified, they are amenable to applied quantum computations that are operationally programmable.

III. SUMMARY

The author has achieved here a brief overview of formalisms within more than ten peer-reviewed published paper articles. Once we recognize that subject areas of classical, quantum, and astrophysics are exceptionally huge, it will become clear why it is impossible to write in gist and understand essence of this subject area in a simple review paper. However, the author has attempted to highlight salient features to make it easier for engineering scientists and technologists to take gist out of all these and apply them intelligently to meaningful products.

It is an earnest effort by the author to elucidate a novel approach to demystify the mathematical complexity of modern physics. Perhaps, the most important point the author would like to shed light on is that discontinuous physics will have to be considered as a serious problem-solving alternative to tackle inconsistencies of quantum physics versus general theory astrophysics. The author has convincingly provided physical reasoning to prove the validity of a rigorous argumentation with discontinuous mathematics having algorithmic graphics, accomplished by gauge physical-mathematical ansatz quantifications.

These algorithmic graphics will be ideal for applying to artificial intelligence machine learning programming that require advancement of syntaxes suitable for quantum computing.

Once these approaches are accepted by experts within Science, Technology, Engineering, Mathematics, andArtistic Management, it is then possible to move further from grueling physics. This will enhance development of productive Apps, AI, and automation IT, that will help to eliminate general human mistakes and errors normally occurring in the design and manufacturing processes.

ACKNOWLEDGMENT

ENGINEERINGINC INTERNATIONAL OPERATIONAL TEKNET EARTH GLOBAL has provided a platform to launch the wonderful ongoing projects that will be most useful to future human progress. Specifically, worldwide Scientists have contributed to the success of the author's peer-reviewed publications as well as group discussions. We have active brainstorming sessions via RESEARCHGATE forums and Zoom Google Meetings. Proceedings of symposia sessions are posted on YouTube @TEKNET EARTH GLOBAL SYMPOSIA (TEGS) website: https://www.youtube.com/channel/UCdU-nenH0oEFiSxivgVqLYw.

With great honor and gratitude, the author would like to thank collaborative international physicists scientists, starting with Emmanouil Markoulakis of Hellenic Mediterranean University, Greece,for hosting visitation to his experimental physics laboratory in 2018 to demonstrate magneton research electron structural mapping breakthrough. Eventually, coauthoring with Emmanouil, the author was able to get into peer publication of ansatz breakthrough sciences to explore and successfully pursue quantum astrophysics. The author would like to thank Christopher O'Neill of Cataphysics Group, Ireland for organizing TEGS meeting conferences every other Saturday with well-reputed physicists at intercontinental earth levels. Special thanks with honor gratitude would go to Manuel Malaver for getting recognized for evolving into astrophysics formalisms. The author would like to extend his profoundly high appreciation to his coauthoring project physicists John Hodge, Wenzhong Zhang, Emory Taylor, and other participating scientists for their highly engaging fruitful debates and discussions. Especially, the author would always be indebted to many upcoming progressive outstanding journals promoting publications with excellent peer-reviews of our papers' articles. These appear essentially in the "*Referential Citations Literature Shortlist*" presented here, although the list is only a sampling!!

REFERENTIAL CITATIONS LITERATURE SHORTLIST

1. Markoulakis E, Konstantaras A, Chatzakis J, Iyer R, Antonidakis E. (2019). Real time observation of a stationary magneton. Results in Physics. 15:102793. https://doi.org/10.1016/ j.rinp. 2019. 102793.
2. Iyer R, Markoulakis E. (2021). Theory of a superluminous vacuum quanta as the fabric of Space. Phys Astron Int J. 5(2):43-53. DOI: 10.15406/paij.2021.05.00233
3. Iyer R. (2021). Physics formalism Helmholtz matrix to Coulomb gage. 6th International Conference on Combinatorics, Cryptography, Computer Science and Computing, November 17-18, 2021, pp.578-588. http://i4c.iust.ac.ir/UPL/Paper2021/accpapers/i4c2021-1001.pdf.
4. Iyer R. (2021). Physics formalism Helmholtz Iyer Markoulakis Hamiltonian mechanics metrics towards electromagnetic gravitational Hilbert Coulomb gauge string metrics. Physical Sciences and Biophysics Journal. 5(2):000195 (9 pages). https://doi.org/10.23880/psbj-16000195.
5. Iyer R, O'Neill C, Malaver M. (2020). Helmholtz Hamiltonian mechanics electromagnetic physics gaging charge fields having novel quantum circuitry model. Oriental Journal of Physical Sciences. 5(1-2):30-48.
6. Iyer R, O'Neill C, Malaver M, Hodge J, Zhang W, Taylor E. (2022) Modeling of Gage Discontinuity Dissipative Physics. Canadian Journal of Pure and Applied Sciences. 16(1). 5367-5377. Publishing Online ISSN: 1920-3853; Print ISSN: 1715-9997.
7. Iyer, R. and Malaver, M. (2021). Proof formalism general quantum density commutator matrix physics. Physical Sciences and Biophysics Journal. 5(2):000185 (5 pages). DOI: https://doi.org/10.23880/psbj-16000185.
8. Fano, U. (1957). "Description of States in Quantum Mechanics by Density Matrix and Operator Techniques". Reviews of Modern Physics. 29 (1): 74–93. Bibcode:1957Rv MP...29...74F. doi:10.1103/Revmodphys.29.74.
9. Iyer, R. N. (2000). Absolute Genesis Fire Fifth Dimension Mathematical Physics. Engineeringinc.com International Corporation. pp.63. ISBN-13: 978-0-9706898-0-1.
10. Iyer R. (2022). Observables physics general formalism. Phys Astron Int J. 6(1):17–20. DOI: 10.15406/paij.2022.06.00244.
11. Iyer R. (2022). A brief overview general formalisms PHYSICS. An Editorial In the Physics & Astronomy International Journal publication processes.
12. Malaver, M., Kasmaei, HD., Iyer, R., Sadhukhan, S. and Kar, A. (2021). A theoretical model of dark energy stars in Einstein-Gauss-Bonnet gravity. Applied Physics. 4(3):1-21.

13. Fano, U. (1995). Density matrices as polarization vectors. Rendiconti Lincei. 6 (2): 123–130. doi:10.1007/BF03001661.
14. Busch, P. (2003). Quantum States and Generalized Observables: A Simple Proof of Gleason's Theorem. Physical Review Letters. 91 (12): 120403. arXiv:quant-ph/9909073. doi: 10.1103/PhysRevLett.91.120403. PMID 14525351. S2CID 2168715.
15. Ardila, L., Heyl, M., Eckardt, A. (2018). Measuring the Single-Particle Density Matrix for Fermions and Hard-Core Bosons in an Optical Lattice. Physical Review Letters. 121 (260401): 6. arXiv:1806.08171. doi:10.1103/PhysRevLett.121.260401.
16. https://www.grc.nasa.gov/www/k-12/rocket/state.html.
17. Rezaei, F., Vanraes, P., Nikiforov, A., Morent, R., Geyter, N. (2019). Applications of Plasma-Liquid Systems. A Review. Materials (Basel). 12(17): 2751. doi: 10.3390/ma12172751.
18. Bialynicki-Birula, I., Bialynicka-Birula, Z. (2021). Time crystals made of electron-positron pairs. Physical Review A 104, 022203.
19. Malaver, M., Iyer, R., Kar, A., Sadhukhan, S., Upadhyay, S., Gudekli, E. (2022). Buchdahl Spacetime with Compact Body Solution of Charged Fluid and Scalar Field Theory. arXiv:2204.00981 [gr-qc].
20. Iyer, R. (2022). Configuring Observables Solving Physical Algorithm Quantum Matrix Gravity. Journal of Modern and Applied Physics, Mini Review, Page 1-5. https://www.pulsus.com/abstract/configuring-observables-solving-physical-algorithm-quantum-matrix-gravity-10507.html.
21. Iyer, R. (2022). Discontinuum Critical Signal/Noise Density Matrix. Physical Science & Biophysics Journal, 6(1):000210.
22. Iyer, R. and Taylor, E. (2022). Rethinking special relativity, spacetime, and proposing a discontinuum. Physics Essays. 35(1):55-60.
23. Hossenfelder, S. (2022). Mathematics Consciousness….
24. Malaver, M., Iyer, R. (2022).Analytical Model of Compact Star with a new version of Modified Chaplygin Equation of State. General Relativity and Quantum Cosmology. https://doi.org/10.48550/arXiv.2204.13108.
25. Iyer, R. (2021). Problem solving vacuum quanta fields. International Journal of Research and Reviews in Applied Sciences. 47(1):15-25.www. arpapress.com/ Volumes/ Vol 47 Issue 1/ IJRRAS_47_1_02.pdf.
26. Denisov, D. and Vellidis, C. (2015).The top quark, 20 years after its discovery. Physics Today. 68(4). Page 46, doi:10.1063/PT.3.2749.

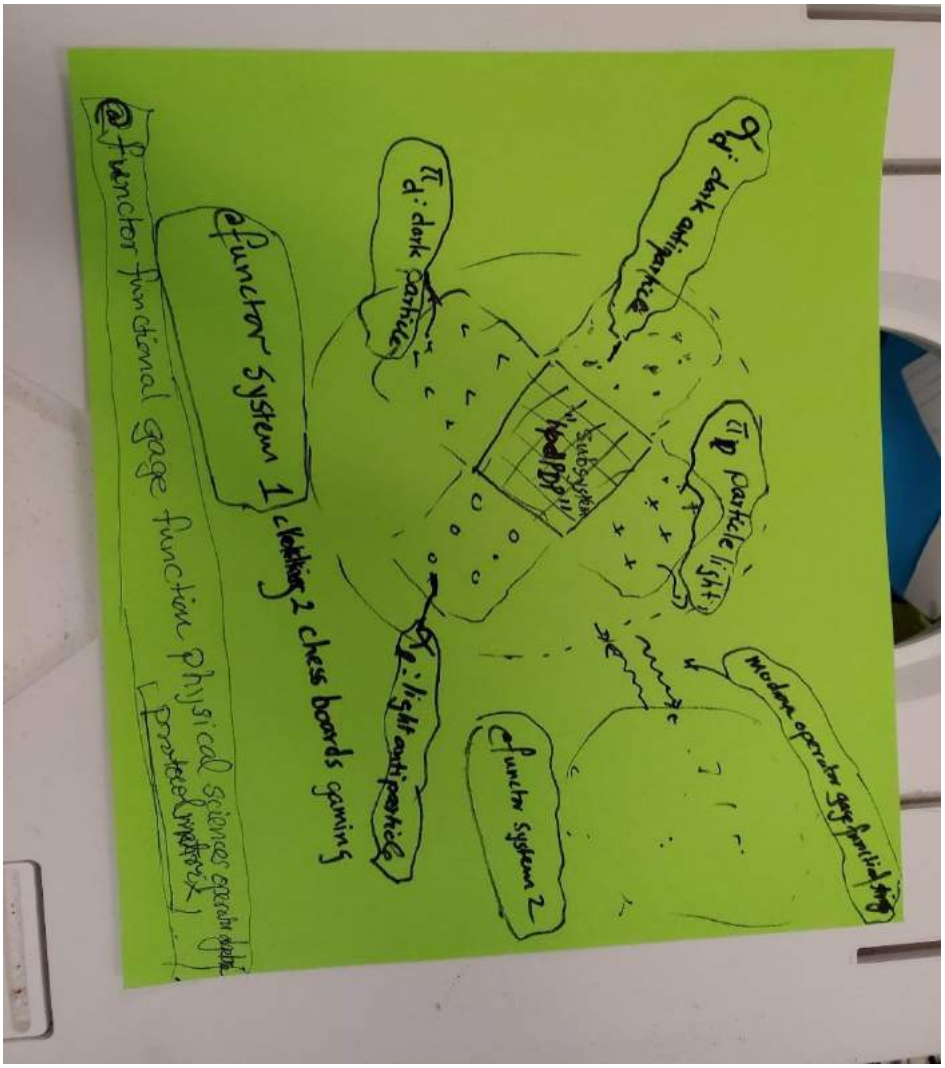

Sketch of scenarios per the article's scheme of PDP, particle, antiparticle, dark-particle, and dark-antiparticle game theory, depicting tic tac chess game perpetual-motion-machine situations. In the background hod-Plenum progenitor Infinitum superluminous aether-type medium implies to provide underlying support base like grounds [6].

PDP progenitor possible mechanism involves dark-bosons and dark-fermions with their antiparticle forms, playing chess tic-tac games shown schematically above. Resultant will appear on the standard zone, which can be guessed to have an observable universe. Regular particle-antiparticle interactions go on; hence, antiparticle particle asymmetry is achievable with hod-PDP circuit mechanism assemblage [5, 6]. Perhaps otherwise, the "CPT" problem prevails, per physics literature. We write a logic algorithm for the formation of gage photons with the phonons that can possibly form in the observable universe {common central standard zone per schema above}, noting that they follow mathematics of the point gradient vortex action fields with their partial differential equations [2, 20, 21].

About gauge algebra functor linked by a functional to function physical Sciences operators

Typical top quark decaying bottom quark [26], playing this scenario game physics dark particle-antiparticle matter would create light phased observable counterparts at the standard zone. They would seem like two chiral antiparallel tops, perhaps asymmetrical, to form a horn-torus electron {Emmanouil Markoulakis's electron model topologically}. Such phenomena have importances top quarks that may be key to know or sense the dark-matter [Sabine Crépé-Renaudin (2018). Dark matter search with the top quarks. Laboratoire de Physique Subatomique et de Cosmologie, Grenoble France.

DM, SUSY, top quark. https://cds.cern.ch/record/2632461/files/ATL-PHYS-SLIDE-2018-551.pdf.]. This knowhow would play key role in understanding antimatter matter action with energy *[*SmartNews article "Tiny Collapsed Star Unleashed a Gargantuan Beam of Matter and Antimatter Reversing Einstein's E = mc^2" https://share.smartnews.com/91tQ8].

0- and 0+ zero-point fluctuations may have relationship to the fine structure constant??!! Area of the absolute vacuum matrix and the string-metrics gage zero matrices = approx. 137??!!

Rider of the pure mathematics of bracket operator mathematics

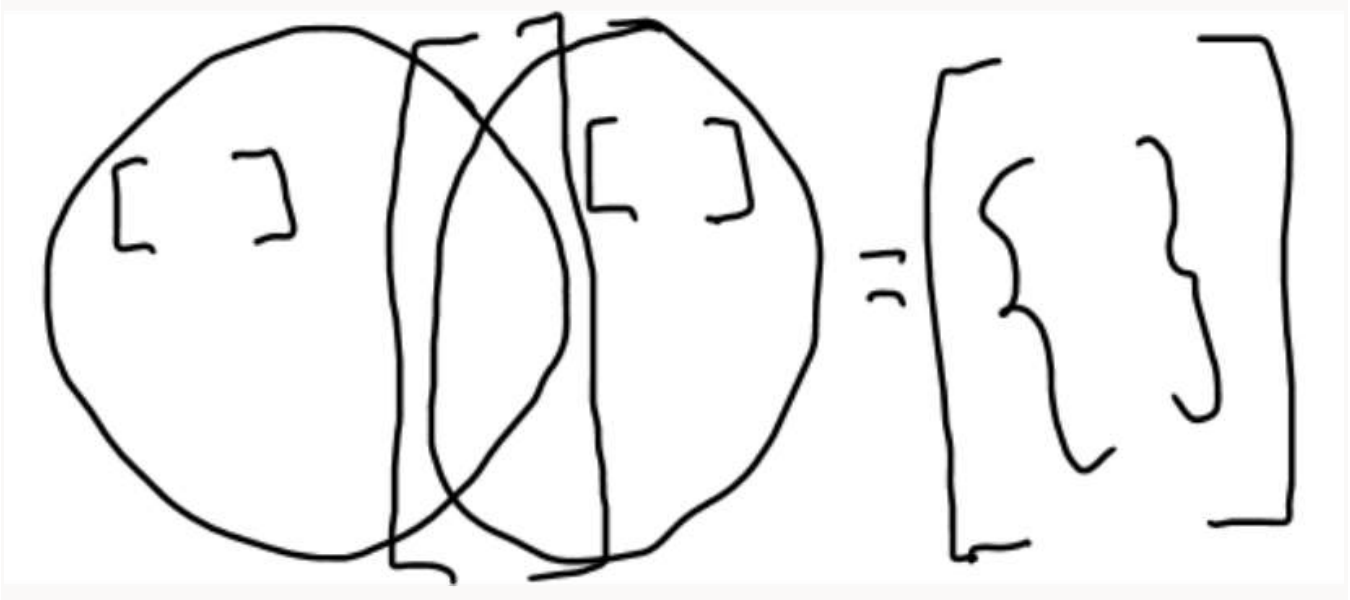

Proof: if { }: set and [ ]: matrix, then [{ }]: matrix contains set;

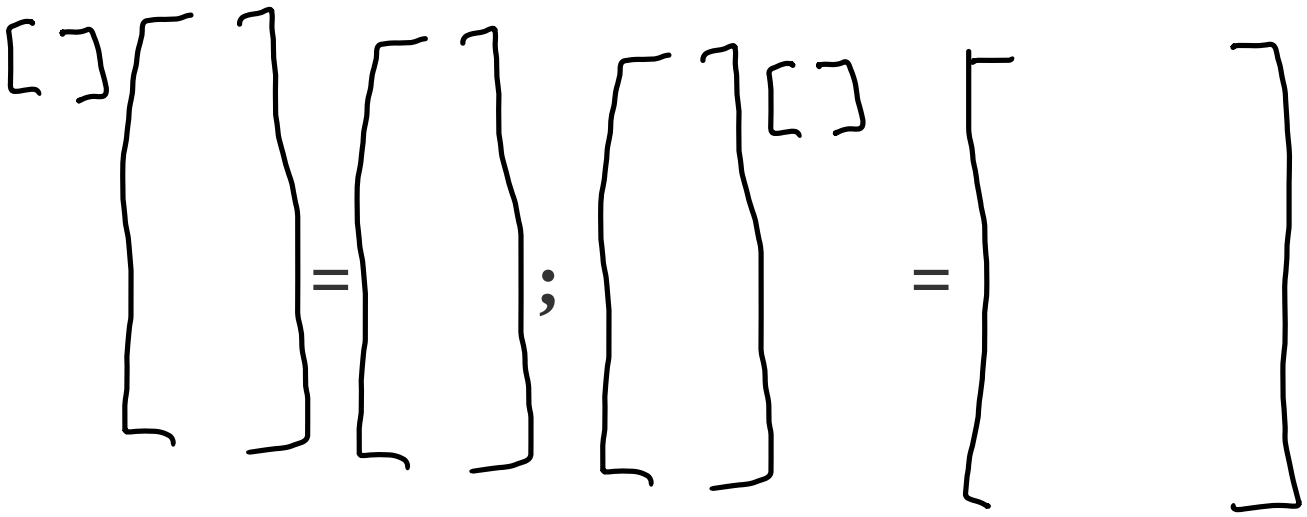

where, 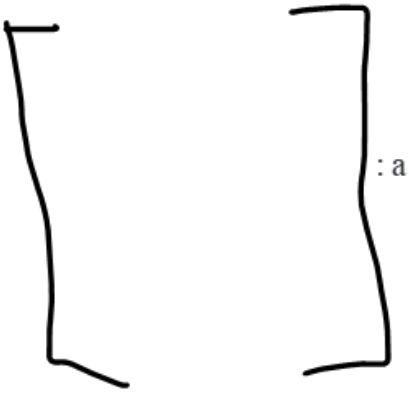 : a density matrix having sets of  .

Therefore, 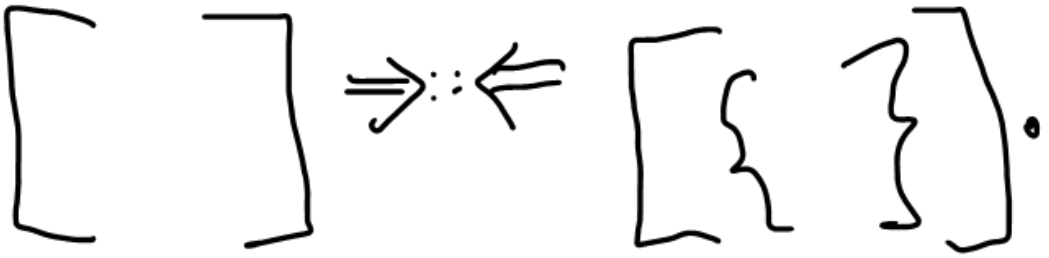

Since 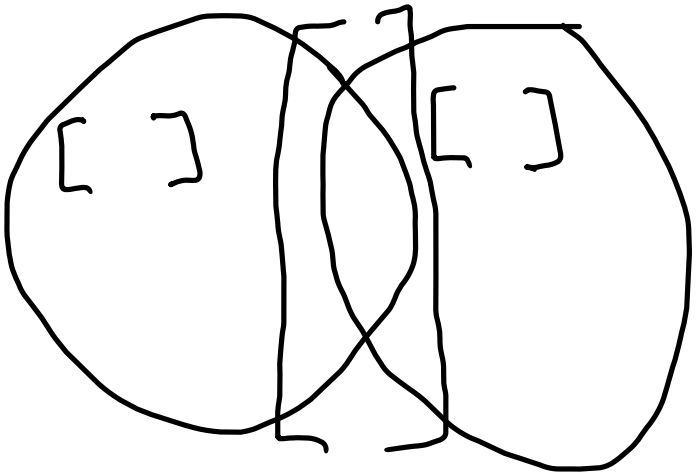 Satisfies all the above definitions having matrix operations with sets within matrix, it is equivalent to

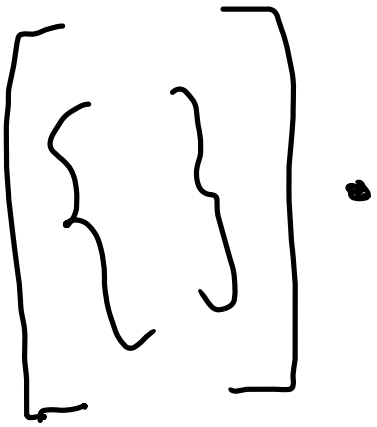

Hence the proof of symbolisms above!! This above proof of the rider of the pure mathematics of bracket operator mathematics would be applicable to situations that involve Venn diagram sets to matrix sets!! Linking logic to language is thus possible!! One such application may be in having symbolic knowledge of the reason of the *Metrix protocol* with closure by removing trivial {matrices, sets} with cancel matrix with quantified mathematical logic per argument derived above.

Example 1: [matrix]{simulating} ><video><" texting" .....communicating.....

= video

{picture of the future} = communicating.....
Audio image video texting communication may be applicable to IT Metrix protocol

Example 2: mathematically [{0}]=0 trivial solution since [{0}]≠0, though 0=0 to similarly, [{g[0]}]≠0, though g[0]=0, per algebraic gage physical mathematical theory author has derived elsewhere. Besides, [{g[0]}]≠[{0}] in types of physics vacuum!!

General solution proof of bracket matrix operator Lagrangian and Hamiltonian algebra:
Let
Point Lagrangian $L_{relativity,point} = p_{relativity}^{2}/2m - \varphi_{relativity,point}$
Point Hamiltonian $H_{quantum,point} = p_{quantum}^{2}/2m + \varphi_{quantum,point}$
If code matrix, **C**[X] = [Y], then for example, [X] = matter mass matrix, m, [Y] = matter momentum matrix, p, and **C** ≡ c, speed of light, these based on signal/noise density critical matrix explained above, $p_{relativity} = m_{relativity}c$; $p_{quantum} = h\, k_{quantum}$. Hence,
$L_{relativity,point} = m_{relativity}c^{2}/2 - \varphi_{relativity,point}$
$H_{quantum,point} = h^{2}\, k_{quantum}^{2}/2m_{quantum} + \varphi_{quantum,point}$
Identification of the problem {φ, m}

Zero-point energy quantum versus relativity must confront {vacuum, ultraviolet} catastrophe. To achieve that, a different approach in terms of the point physics has been achieved already by the author working with coauthoring international scientists, listed @ "Referential Citations Literature Shortlist".

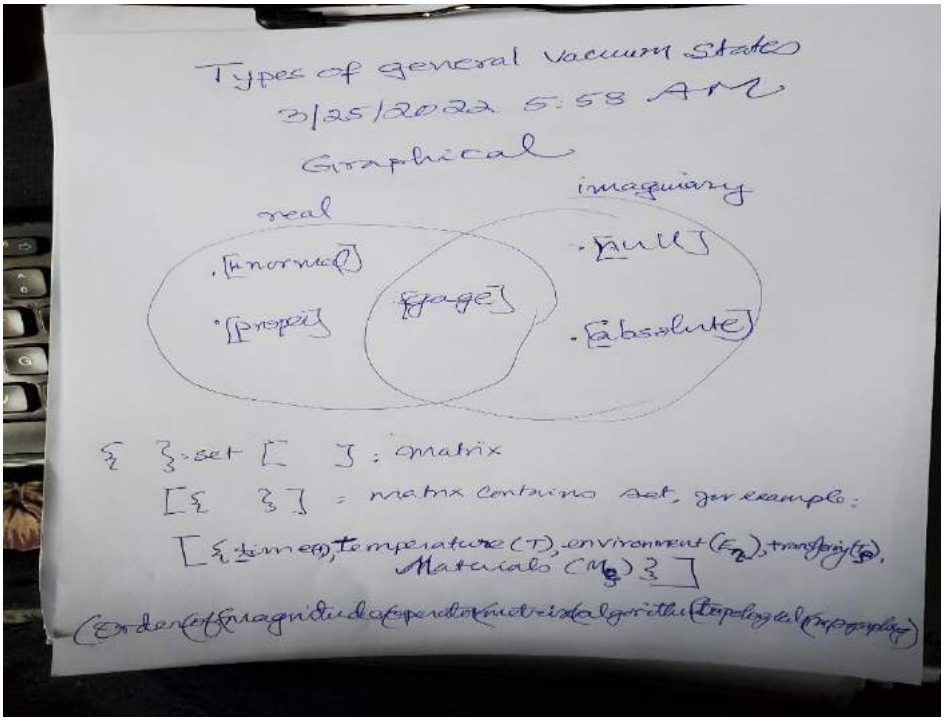

Gage zero-point fluctuations absolute zero vacuum matrix switching with zero metrics gage string-metrics matrix entropic vacuum essentially.

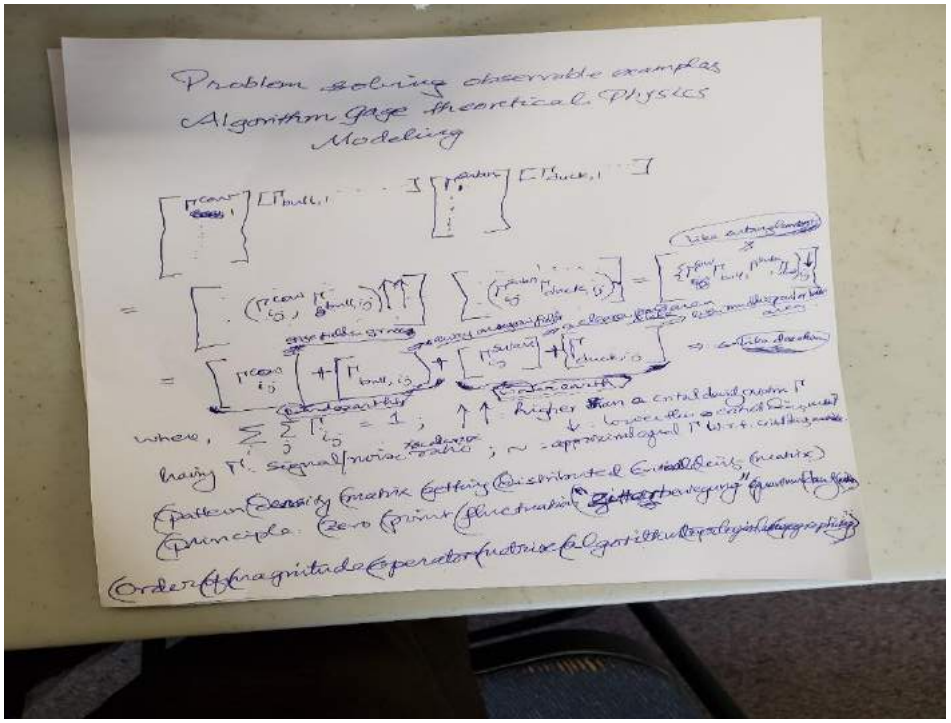

Proof observations are verifying the PDP circuit assembly physics with mechanism observables. Order magnitude gets acceptable towards verifying dark matter energy entity experimentally.